DRAFT DRAFT

REPORT ON LAKE AND SHORE ICE CONDITIONS ON SOUTHEASTERN LAKE MICHIGAN IN THE VICINITY OF THE DONALD C. COOK NUCLEAR PLANT: WINTER 1974-75

by

Erwin Seibel, Christopher T. Carlson and

Joseph W. Maresca, Jr.

May 1977

ABSTRACT

A time-lapse photographic system was used to provide a nearly continuous record of ice conditions along a segment of the southeastern Lake Michigan shoreline during the 1973-74 and 1974-75 winter seasons. By analysis of the photographs for both seasons, the ice conditions were catagorized into five distinct stages of evolution from formation through breakup and a typical sequence of nearshore ice formation was identified. From the photographic record of nearshore ice conditions, a three-element mechanism for the development of the nearshore ice ridges in the vicinty of the study site was formulated. Quantitative analysis of the photographs was used to test and subsequently verify the hypothesis that the nearshore ice ridges, offshore bars and breaker zones are coincident in location. Observations reveal that large quantities of sediment are incorporated into the nearshore ice during formation and that the nearshore ice ridges are grounded on the offshore bars.

The two year ice condition record was correlated with local climatological data to evaluate the relationship existing between the two. The five phase model of nearshore ice status displayed a complex interrelationship with wind direction, wind speed, and air temperature.

We believe that the grounded nearshore ice ridges simultaneously modify the nearshore topography and effectively protect the shoreline and bluffline from erosion by winter storms. The degree to which the nearshore is protected or modified has not yet been established.

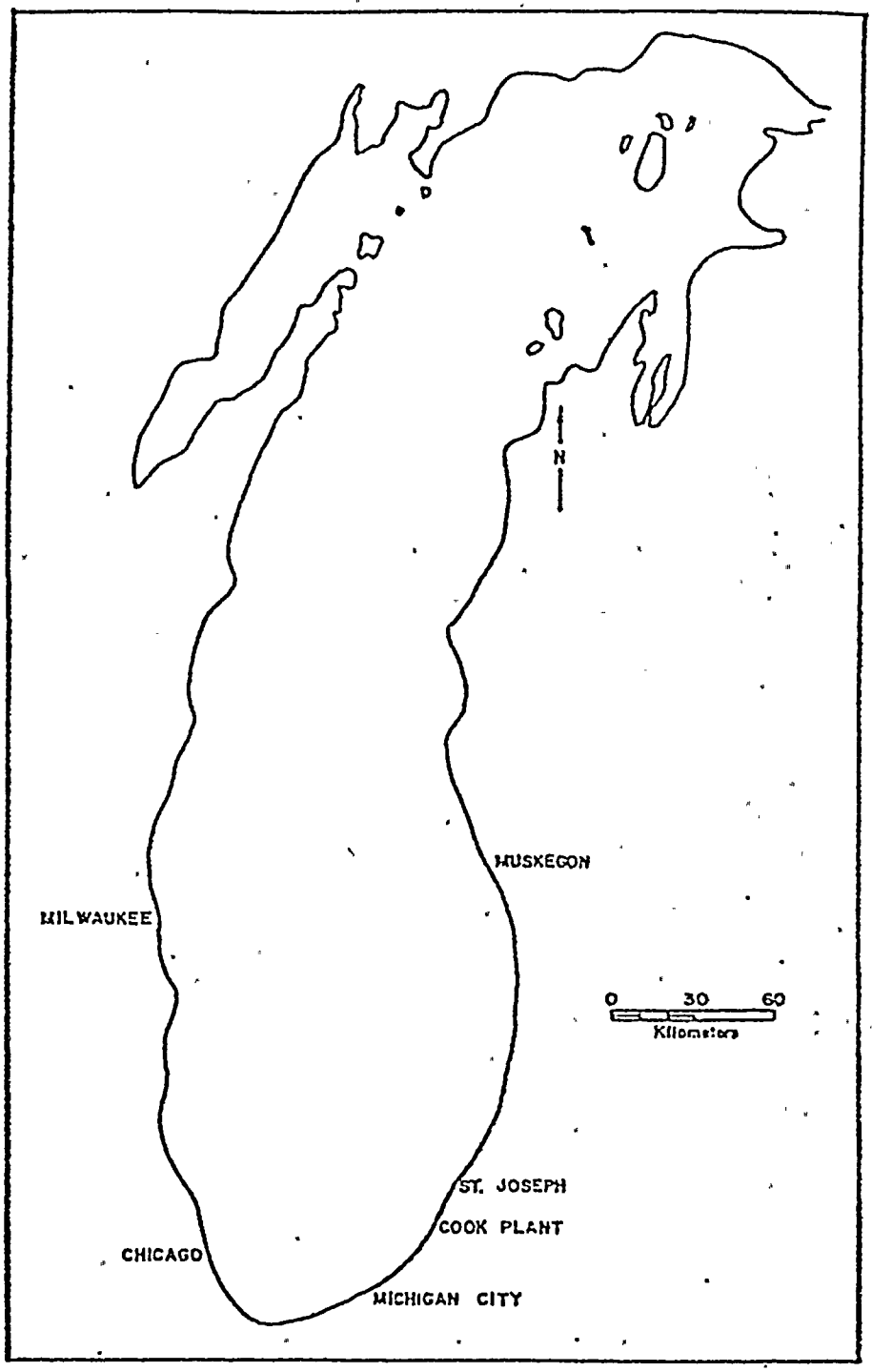

FIGURE 1. Location of the Donald C. Cook Nuclear Plant.

METHODOLOGY

High oblique photographs were obtained for analysis with a Canon F-1 single reflex 35 mm camera with Canon 50 mm f 1.8 lens. The camera with Canon Servo EE Finder and special timing unit was mounted indoors facing in a NNW direction and automatically provided an average of five photographs per day from early morning to late afternoon. Since it was not possible to determine the exact time of exposure for each slide, a relative time was assigned to each photo: early a.m., late a.m., noon, early p.m., and late p.m. The positions of a sheet pile seawall and a range pole, evident in each photograph, were determined by standard field survey methods and were used as reference points. The camera location permitted observation of isolated ice blocks as well as cross-sectional ice ridge profiles visible through wave-breached portions of the ridge system. In each slide the horizon was evident. Reflected glare from the lake surface, ice, or window glass did not interfere with the quality of the photographs.

Slides were selected for use in the analysis instead of prints for two reasons. First, slides are less expensive to process than prints; and second, analysis required that the images of variables in the oblique photographs be marked on a tracing paper overlay. Slides were easily enlarged with a slide projector to minimize human error in selecting points from the image.

Representative slides or groups of slides were chosen for analysis from the sequence taken during the period from 12 January 1975 through 24 March 1975 (Appendix A). These dates are respectively the date of initial ice formation and final melt-off of all isolated remnant ice blocks.

Analysis of the slides was divided into three steps. First, points were marked locating the positions of variable features in the projected oblique representation, and their coordinates were determined relative to an (x,y) coordinate system with origin at the principal point of the oblique photograph. Second, the positions of these points were calculated for the equivalent vertical photograph with coordinate system origin at its isocenter. Finally, the real ground coordinate positions of the points were determined relative to a coordinate system with origin at the camera. The geometry basic to this method of oblique photograph analysis is discussed under *Geometry of oblique photographs.*

A fixed reference system was requisite for slide-to-slide comparisons. Establishment of such a coordinate system with origin at the principal point of the projected oblique photograph necessitated the removal of the color transparency from the developer's cardboard mount and remounting on a 2.0 inch plexiglass square as suggested by Maresca (1975). Inscribed on the plastic mount were a series of lines parallel to its borders to aid in placement of the positive. Also etched on the mount were the fiducial axes whose origin is located at the principal point of the remounted color transparency.

The remounted slide was projected by a Kodak Ektagraphic slide projector onto a wall covered with a tracing paper overlay. The projected image of the fiducial coordinate axes, now superimposed on the projected photograph, was located on the overlay. To minimize error due to remounting, the location of the projected principal point was checked and adjusted when necessary.

The perpendicular distance was measured between two of the inscribed horizontal lines of the plastic mount, one at the top and one at the bottom

of the mount. The distance between the projected image of these two lines was measured on the screen, and these values were used in the computer program for calculation of the focal length of the projector. The positions of the reference points common to all slides were marked on the overlay and subsequently the projected positions of the variables unique in each slide were located. These variables included the horizon, breaker zones, ice ridges, inter-ridge ice lagoons, zones of brash ice accumulations, heights of the icefoot, ice blocks, and ice ridges as well as the waterline when visible.

The computer program utilizes the mean still water level (MSWL) as the datum for ground coordinate calculations thus requiring that the selected data points be located at this elevation. When possible, points defining variable positions were therefore marked on the tracing paper overlay where their intersection with the water surface was evident in the projected picture. The points marking the location of breaker zones were placed at the base of the breaking waves. Points marked along the crest of an ice ridge, above the MSWL datum, would represent only an estimate of the ridge's position (see Appendix C). Consequently, when determining ice ridge location, it was frequently necessary to use a later slide which depicted the breaching of, or breakup of that ice ridge when its intersection with the water surface at mid-ridge was visible. At the time of this mid-ridge exposure, the height of the ridge crest above the MSWL could be determined with the assistance of computer program HEIGHT. Assuming a slow melting rate resulting in minimal reduction in ice ridge relief, the computed height could then be used to compute the ground coordinates of the ice ridge in preceding photographs when only the ice ridge crest was visible. The elevations of the

control points, which were not located at the MSWL, were determined using standard field survey methods and utilized directly in computing their ground coordinates. Points defining the outline of brash ice areas of the edges of the inter-ridge ice lagoons were in most cases considered to be at the MSWL.

The distance from the principal point of the oblique photograph to the apparent horizon is utilized in the program for calculation of distances on the principal plane diagram, hence, the position of a poorly defined horizon may introduce errors. The quality of the horizon was evaluated as excellent, good, fair, or poor, thus offering one possible explanation of error in poor computer output values.

The cartesian coordinates of the points locating the positions of variables on the projected oblique photograph were obtained using a coordinate grid and dial calipers. The tracing paper overlay on which the data points were marked was placed over the coordinate grid and the data point coordinates determined to the third decimal place.

The computer program ICE75 converts the oblique (x,y) coordinate points to equivalent vertical photograph coordinates and then calculates the real ground coordinates for each ordered pair. The real ground coordinates as calculated in subroutine PHOTO are supplied to subroutine REGRES where a regression line is fit to each linear array of coordinate points marking the location of a given monitored variable. Digital plotting subroutines called in the main program construct and label a cartesian ground coordinate grid with origin centered at the camera. Computed ground coordinates for each data point were scaled and plotted within the coordinate grid. A

unique plotted character was used for each monitored variable. Characters respresenting the location of each variable were positioned in linear arrays on the plotted grid (Appen. C) and each regression line was plotted through its respective array of data points. The distances to all variable positions were calculated perpendicular to a baseline along the shore. The sheet pile seawall was chosen as the baseline since the waterline is subject to frequent changes in position and is usually not visible during periods of ice cover. Presently, the computer program does not calculate the distances from the baseline to the various variable positions. All distance measurements were made perpendicular to the baseline from each of three selected points (see Appendix C). Normals to the baseline were contructed at these three points of sufficient length to intersect the lines defining the variable positions. Each normal formed the hypotenuse of a right triangle. Determination of the x and y components of the baseline normal and application of the plotting scale factor and the Pythagorean Theorem yielded distances to the variable's location. This technique was used to calculate the distances from the baseline to all monitored variables.

GEOMETRY OF OBLIQUE PHOTOGRAPHS

Techniques for the analysis of an oblique representation can be obtained from any standard photogrammetry text, but is presented here briefly so that the correction for the projection of the image through a slide projector may be included. The geometry of the principal plane diagram (Olson, 1973) (Figure 2) was used to derive the fundamental equations required to analyze the oblique photograph. The distance PX is measured on the screen from the principal point of the photograph to the apparent horizon. Since this distance is projected onto a screen from a slide projector, the image distance must be corrected for the focal length of the slide projector. A constant, C, is used to make this correction . The constant, C, is defined as

$$C = I/O \tag{1}$$

where I is the image distance and O is the object distance. The image distance, I, may be calculated from the lens maker's formula

$$I = O x f_{proj}/(O-f_{proj}) \tag{2}$$

where f_{proj} is the focal length of the projector. The distances on the principal plane positive can now be define. The angle of depression, θ^1, is defined as

$$\tan \theta^1 = PX/f_{cam} \tag{3}$$

where

$$PX = PX_{screen} \times C \tag{4}$$

and cam is the focal length of the camera. The distance PX and the angle θ^1 were calculated to the apparent horizon. A small correction must be made to determine θ^1 to the true horizon by adding

$$\theta = 0.98 \quad H \tag{5}$$

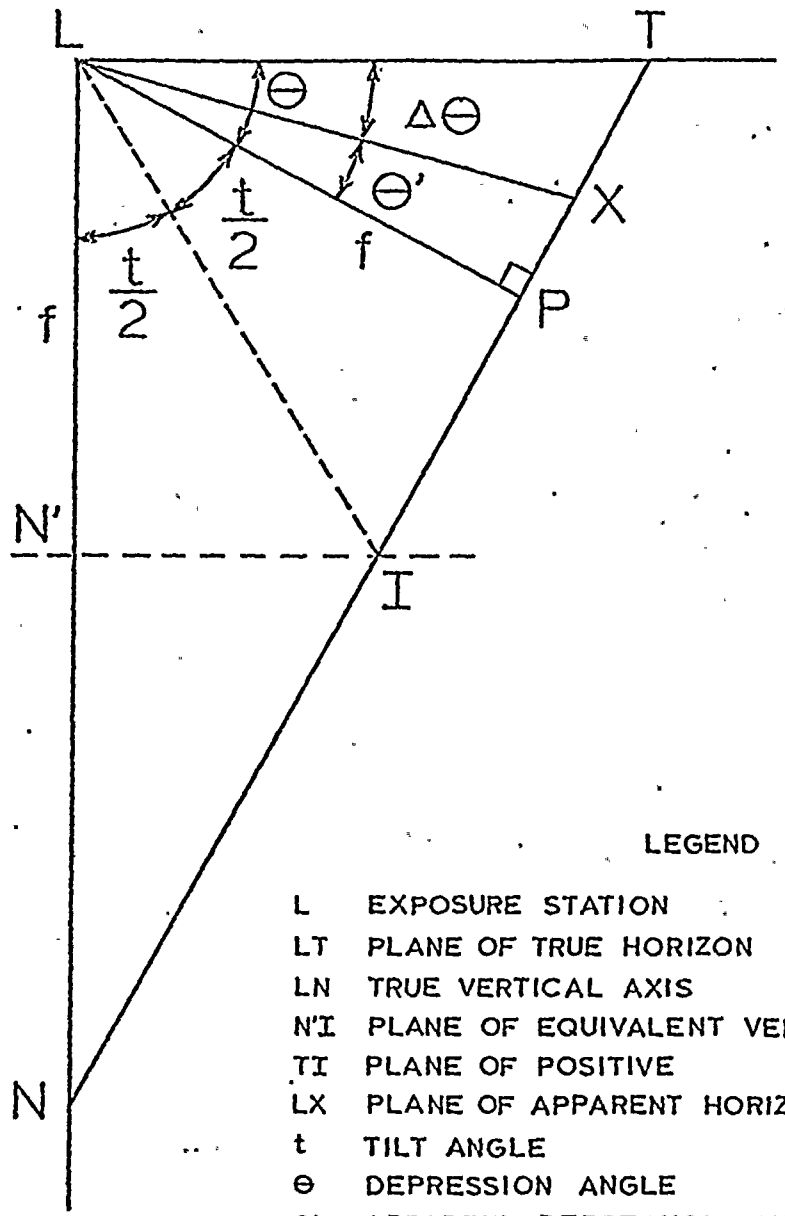

LEGEND

L	EXPOSURE STATION
LT	PLANE OF TRUE HORIZON
LN	TRUE VERTICAL AXIS
N'I	PLANE OF EQUIVALENT VERTICAL PHOTOGRAPH
TI	PLANE OF POSITIVE
LX	PLANE OF APPARENT HORIZON
t	TILT ANGLE
θ	DEPRESSION ANGLE
θ'	APPARENT DEPRESSION ANGLE
Δθ	DIP ANGLE

FIG. 2. Principal plane diagram.

$$X_{grd} = H \times X_{v.p.} / f_{cam} \quad (13)$$

$$Y_{grd} = H \times (PI + Y_{v.p.})/f_{cam} \quad (14)$$

The fundamental assumption basic to the analysis is that all points lie within the datum plane. If a point lies outside the datum, as for example a point on the crest of an ice ridge, then a different elevation, H, must be used. Vertical elevations or vertical heights were calculated in the computer program HEIGHT using the formula

$$h = H \times (d/r) \times (TN/TS) \quad (15)$$

Two computer programs, ICE75 and HEIGHT, were written for the analysis of high oblique photographs using the above formulae. Program HEIGHT may be used to determine the height of an object above the datum if the elevation of at least one point on the object is known. The object height calculated by program HEIGHT may be used in program ICE75 to convert from oblique to the real ground distances. The output was produced in both tabular and graphical format. The locations of the breaker zone, waterline, baseline and ice ridges were determined and the height of ice ridges was calculated when a cross-section of the ridge was visible in the photo.

in minutes to θ^1, where H is the height of the camera above the datum and θ is the dip angle. Since $\theta = \theta^1 + \theta$, the distance PT must be calculated. The geometry of the principal plane diagram (Figure 2) may be used to derive the distance PI using

$$PI = (\tan t/2) \times f_{cam} \tag{6}$$

where t equals 90 - θ. The remaining distances in the principal plane diagram are given in equations 7, 8, and 9.

$$PN = f_{cam} \times (\tan t) \tag{7}$$

$$TI = PT + PI \tag{8}$$

$$TN = PT + PN \tag{9}$$

Using this information, all points in the oblique representation can be rotated into an equivalent vertical photograph and finally real ground distances are obtained.

Individual ordered pairs, (X_{scrn}, Y_{scrn}), are picked off the oblique photographic projection on the screen relative to a rectangular coordinate system with origin at the principal point. The coordinates, $(X_{v.p.}, Y_{v.p.})$ of the equivalent vertical photographs are calculated as

$$X_{v.p.} = X_{scrn} \times C \times (TI/\ [TI-K]) \tag{10}$$

$$Y_{v.p.} = K \times (TI/\ [TI -K]) \tag{11}$$

where

$$K = (Y_{scrn} \times C) + PI \tag{12}$$

The real ground coordinates, (X_{grd}, Y_{grd}), can be calculated from a simple proportion between the equivalent vertical photograph and the ground relative to a rectangular coordinate with the origin at the camera. The coordinates (x_{grd}, Y_{grd}) were calculated using

ICE RIDGE LOCATION AND NEARSHORE TOPOGRAPHY

Seibel et al., 1975, showed that the location of breaker zones and ice ridges is coincidental. The data collected during January and February 1975 further substantiate these findings.

Using the high oblique photographs for the winter of 1975, we measured the distance from a permanent baseline to the breaker zones and ice ridges. The measured points are shown in Figure 3 and their values are recorded in Table 1. Three breaker zones and three ice ridges were identified during the 1974 winter season. However, only two ice ridges were visible in 1975. The 1974 and 1975 data have been plotted together in Figure 3. The correlation between breaker zone and ice ridge location is smallest for the first breaker zone and ice ridge. Coincidence between the ice ridges and breaker zones is still present further offshore, but the scatter of the data points is greater.

The scatter in the data is a function of the analysis and the real variability in the mean position of the ice ridge, breaker zone, and nearshore bars. Each variable is positioned within a linear zone and its location is approximated by a line for measurement purposes. In particular, the breaker zone (offshore bar) has a natural width and since its location is defined by only one slide at a given time, this location is dependent upon wave conditions as well as the position of the breaking wave at the time of photograph exposure. It follows that one photograph at any given time is not sufficient to define the range in width of this zone.

The second offshore bar is wider than the first (Davis and McGeary,

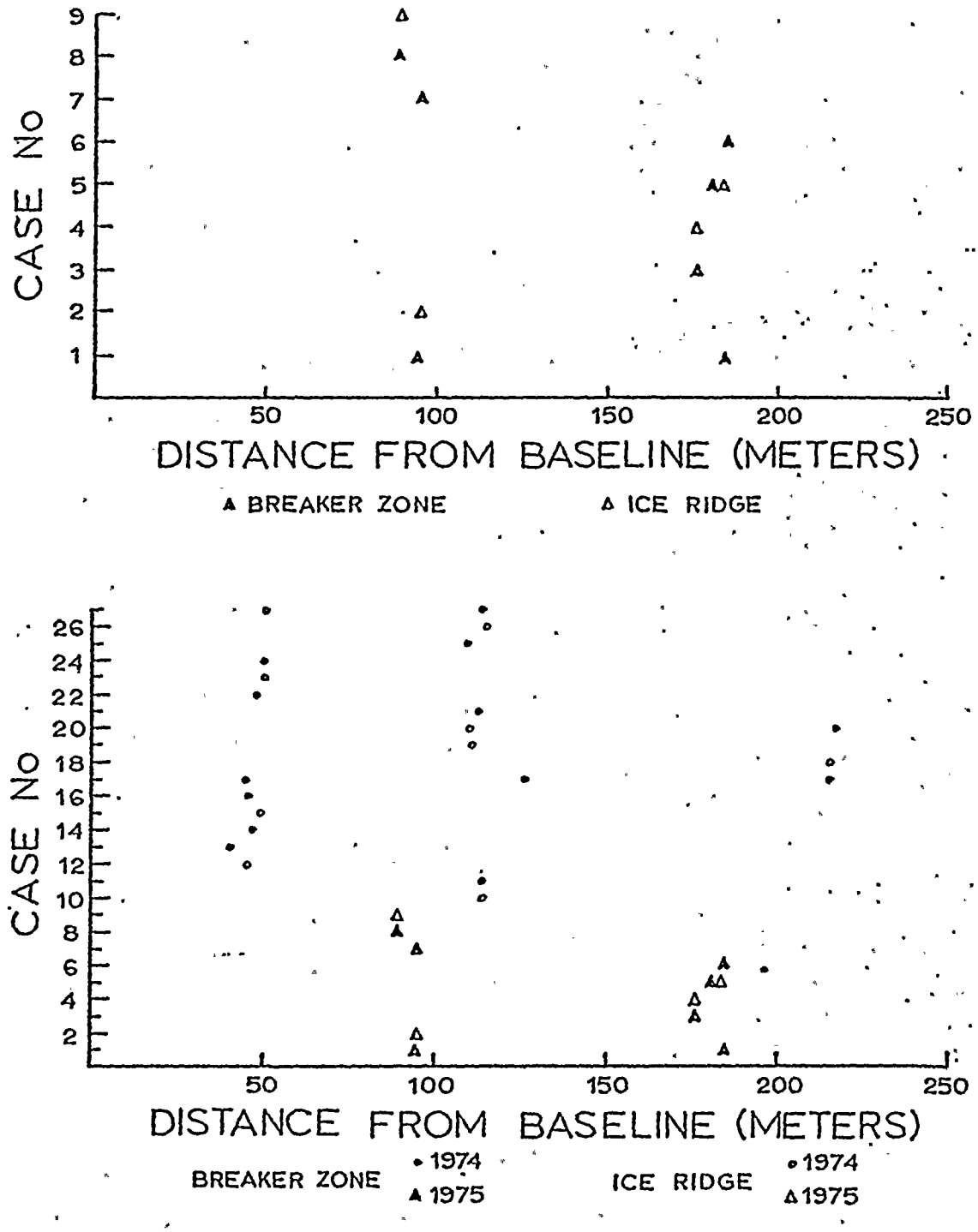

FIG. 3. Plot of the location of breaker zones and ice ridges for the analyzed photographs for the years 1974 and 1975.

TABLE 1. Identification of the case numbers used in Figure 3

Case	Slide No.	Date	0-100 Meters		101-200 Meters		201-300 Meters	
			Breaker Zone	Ice Ridge	Breaker Zone	Ice Ridge	Breaker Zone	Ice Ridge
1.	CM-01-75-08	1-12-75	94		184			
2.	CM-01-75-12	1-13-75		95				
3.	CM-01-75-18	1-14-75			176			
4.	CM-01-75-20	1-15-75				176		
5.	CM-05-75-37	2-25-75			182	184		
6.	CM-06-75-01	2-25-75			185			
7.	CM-06-75-21	3-01-75	95					
8.	CM-09-75-02	3-22-75	89					
9.	CM-09-75-02	3-22-75		89				
10.	CM-09-74-23	1-17-74				114		
11.	CM-10-74-02	1-22-74			114			
12.	CM-10-74-03	1-22-74		45				
13.	CM-10-74-09	1-23-74	41					
14.	CM-10-74-18	1-24-74	47					
15.	CM-10-74-20	1-25-74		49				
16.	CM-10-74-29	1-27-74	46					
17.	CM-11-74-13	1-31-74	45		127		215	
18.	CM-13-74-19	2-15-74						216
19.	CM-13-74-26	2-17-74				112		
20.	CM-14-74-02	2-19-74				110	218	
21.	CM-14-74-03	2-19-74			113			
22.	CM-12-74-12	2-07-74	48					
23.	CM-12-74-29	2-10-74		50				
24.	CM-14-74-16	2-22-74	50					
25.	CM-14-74-34	2-25-74			109			
26.	CM-14-74-36	2-26-74				115		
27.	CM-17-74-03	3-13-74	51		113			

1965), thus providing greater latitude for the location of breaking waves and ice ridges. The position of an ice ridge is more definitive since grounded remnant ice blocks (Figure 4d) maintain their position during breakup. Frequently wave activity breaches an ice ridge providing a cross-sectional view and revealing its mid-ridge intersection with the water surface. This breached cross-section maintains its position in several slides allowing calculation of both the ice ridge's position and height.

Offshore profiles were taken before and after the winter ice formation in both 1974 and 1975. The 1974 profiles indicated offshore bars at approximately 116 m, and between 230 to 270 m from the baseline. Profiles following the ice season in 1975 showed the offshore bars had relocated at approximately 180 m, 335 m, and 610 m. The location of the second bar in the profiles shows good agreement with the data for the respective year, although these distances were not used in the correlation. The soundings, taken at 30.5 m intervals, missed the first bar and were too widely spaced to define the other offshore bar locations with the required precision.

The position of the breaker zones is known to reflect the position of the offshore bar system. The clear relationship between the offshore ice ridges and the breaker zones leads to the conclusion that ice ridges are coincidental with the bar systems. The time-lapse photographs of the nearshore ice complex indicate that once established the ice ridges remain stationary for longer periods than the intervening lagoons. This suggests that not only are the ice ridges greater in thickness than the ice lagoons but that they are situated directly on the nearshore lake bottom. O'Hara

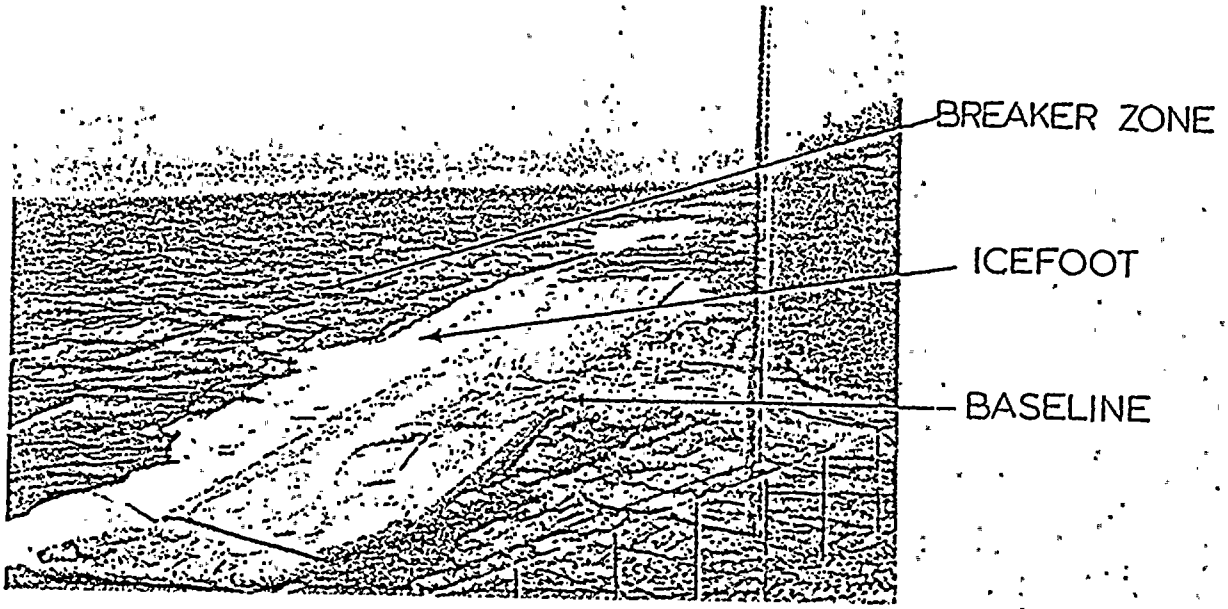

a) The baseline, icefoot and first breaker zone.

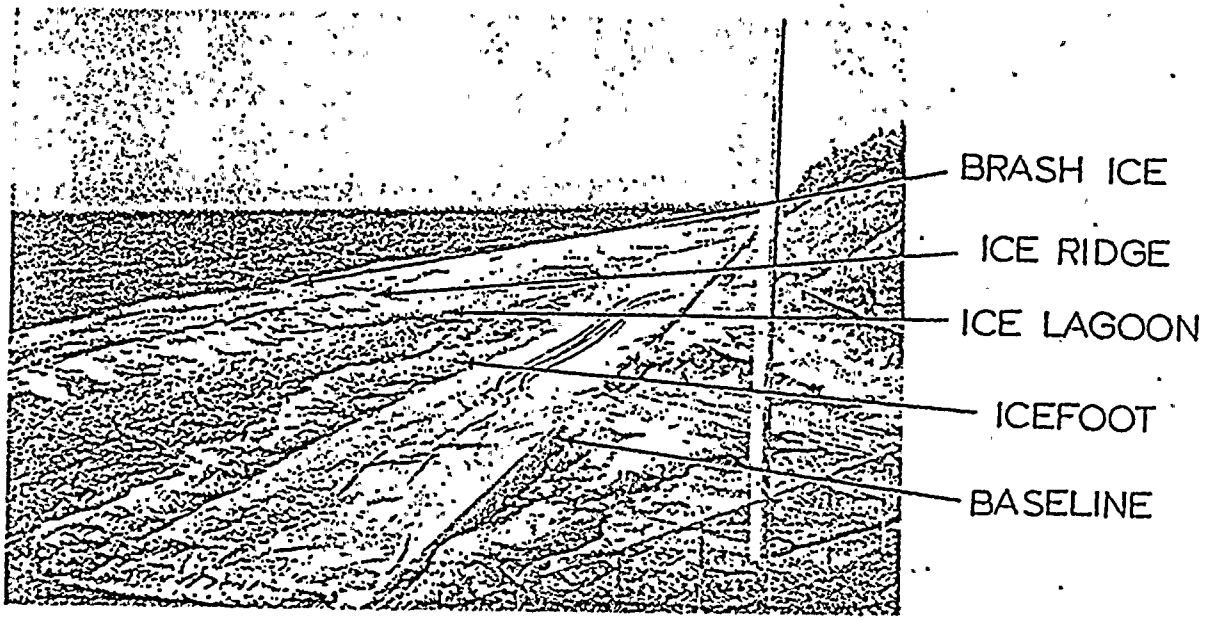

b) The baseline, icefoot, first ice lagoon, first ice ridge and floating brash ice.

FIG. 4 . Characteristic ice features at various stages in the formation and breakup of the nearshore ice complex.

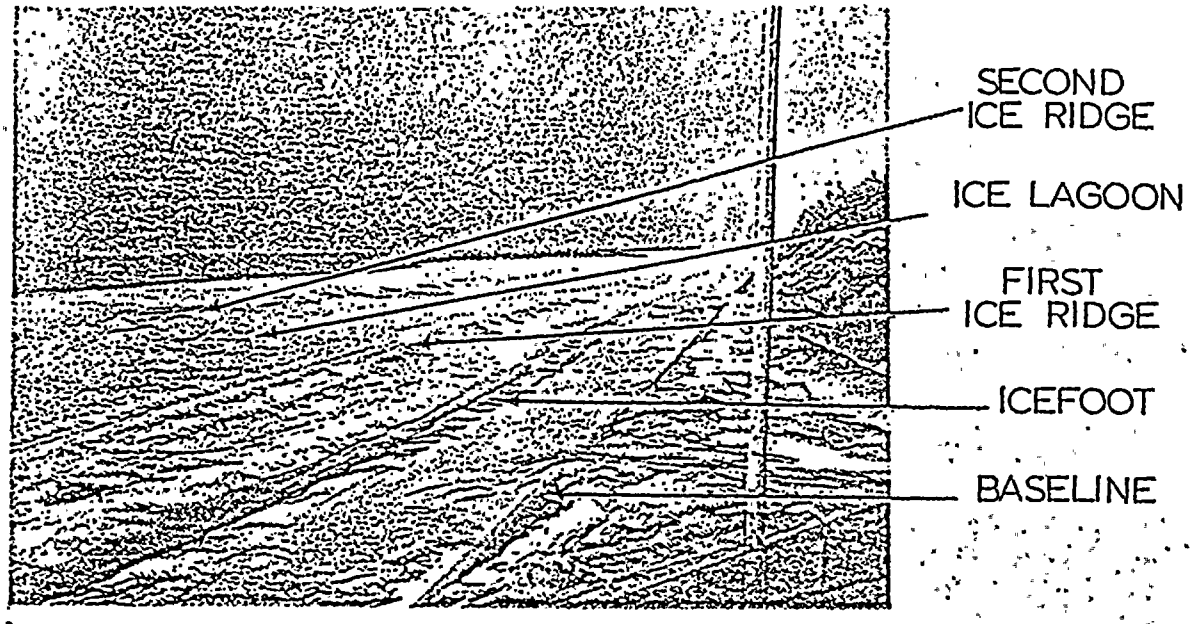

c) The ice complex from shore to beyond the second ice ridge.

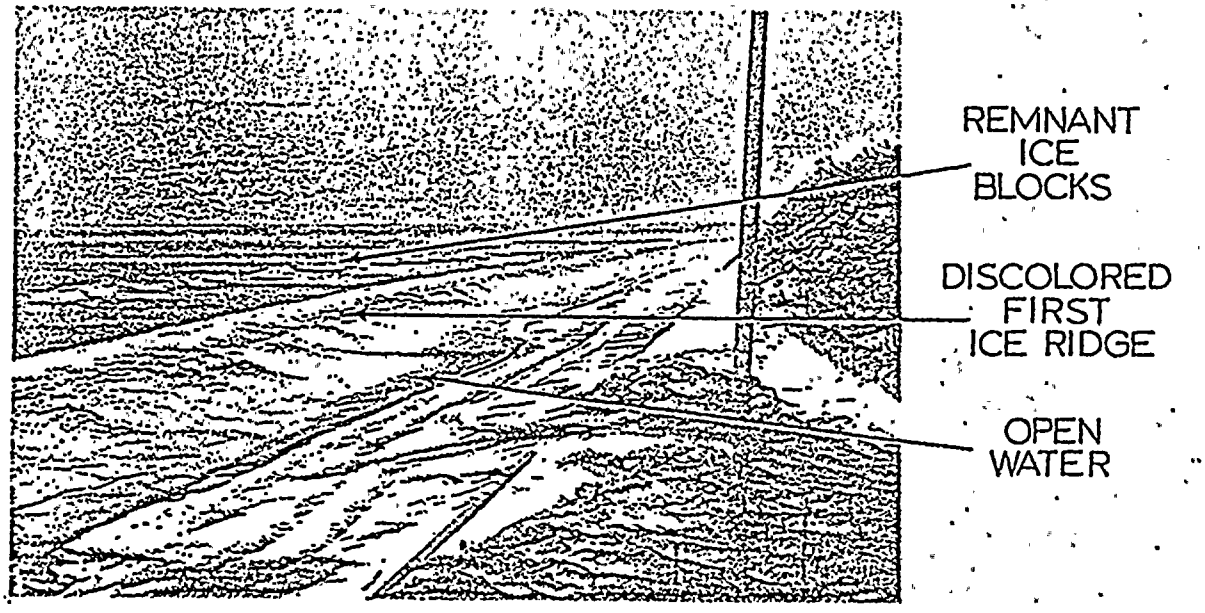

d) Remnant ice blocks delineating the former position of the second ice ridge.

FIG. 4 continued.

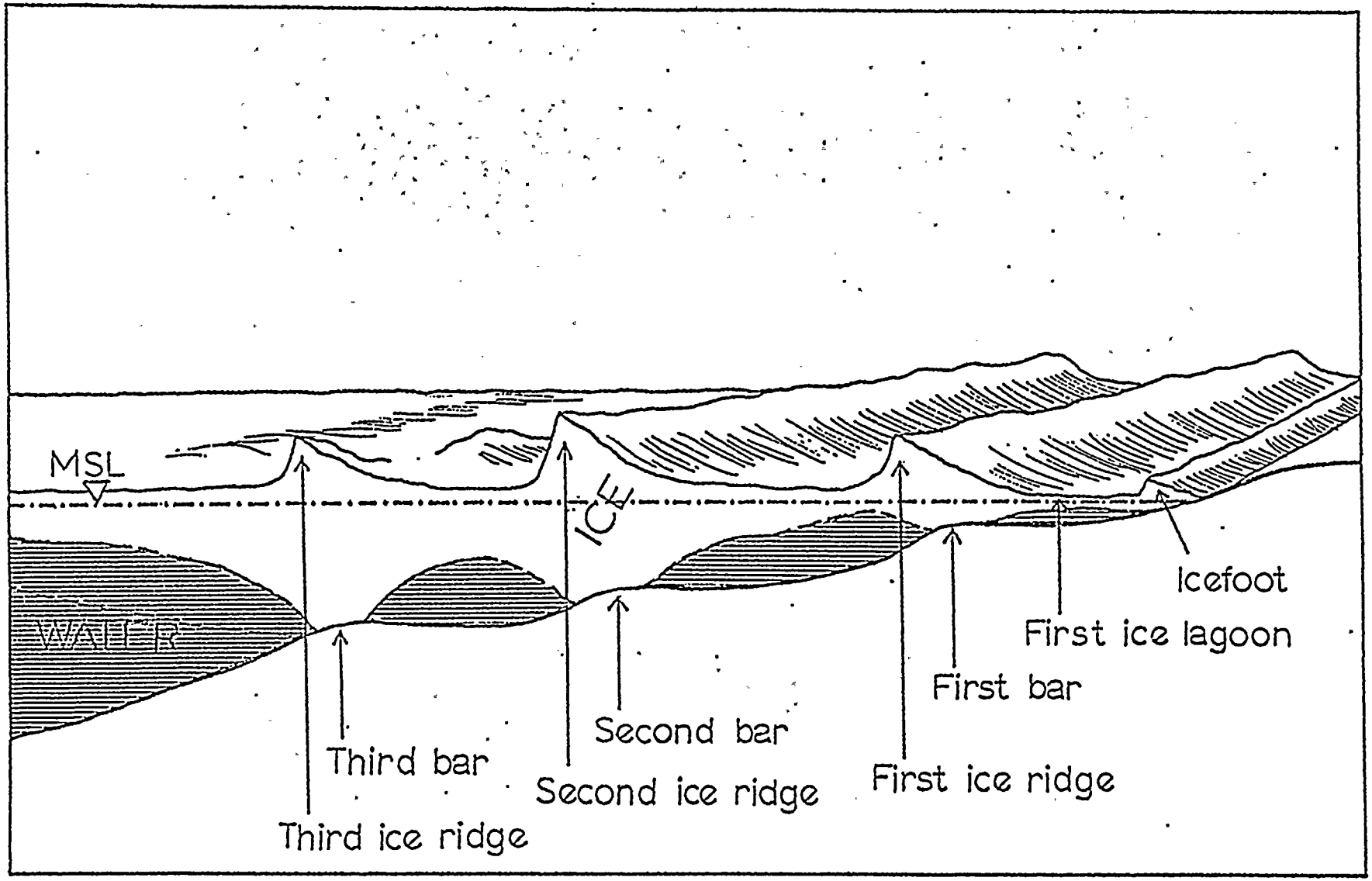

FIG. 5. Schematic representation of the typical nearshore ice complex at the study site.

and Ayers (1972) verified during diving operations that the remnant blocks of a deteriorating ice ridge were embedded on the bottom. Bryan and Marcus (1972) observed remnant ice blocks grounded along offshore bars during an aerial reconnaissance.

ICE CONDITIONS: CLIMATOLOGICAL DEPENDENCE

The ice conditions were categorized into five distinct stages: no ice, accretion, static, deterioration, and breakup. The stages of ice development used here were determined from the time-lapse photography of the ice at the study site. Accretion is a visible addition of ice since the time of the previous slide while deterioration and breakup are a reduction in the ice mass. Deterioration is a gradual reduction of the ice mass apparent only after a series of slides is viewed in succession while breakup is the rapid destruction of the nearshore ice complex usually under severe lake conditions. During breakup, rapid change is visible from slide to slide and is usually exemplified by the landward displacement of the ice complex. The static condition referred to here connotates no visible change in the ice complex from slide to slide.

The stages of ice development were related to the following climatic conditions: wind direction, wind speed, air temperature, and water temperature. Figures 6 through 12 and Appendix D show the climatic conditions as they relate to the ice conditions for January, February, and March 1975. It becomes apparent that no single climatological variable fully controls the ice development at all times. The combined influence of air temperature, wind direction, and wind speed determine the stages of ice development in a complicated manner.

Water temperature has the least influence on ice conditions. Although the water temperature data has been tabulated in Appendix D , its correlation with the ice condition is poor and hence these have not been

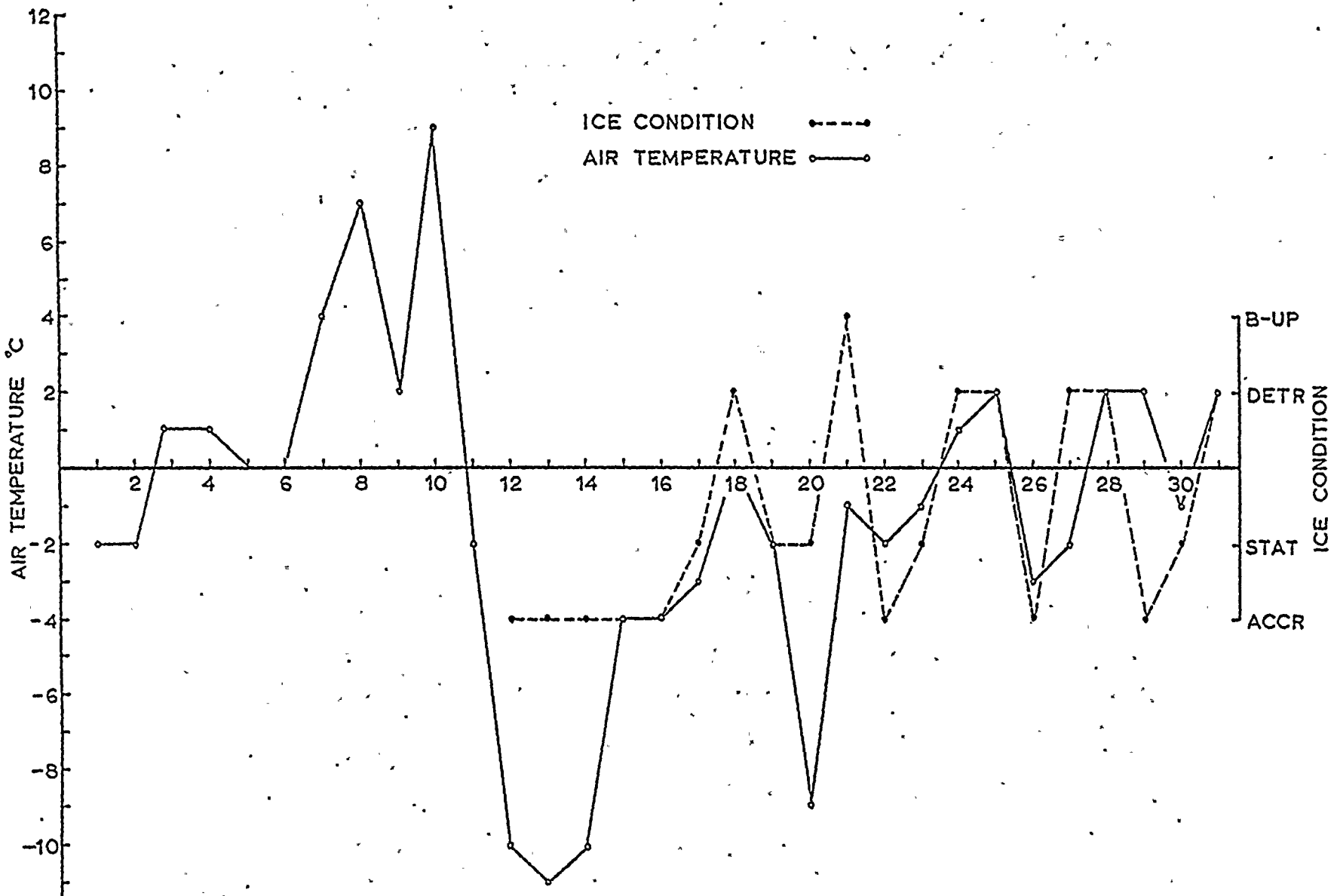

FIG. 6. Daily mean air temperature and ice conditions: January 1975

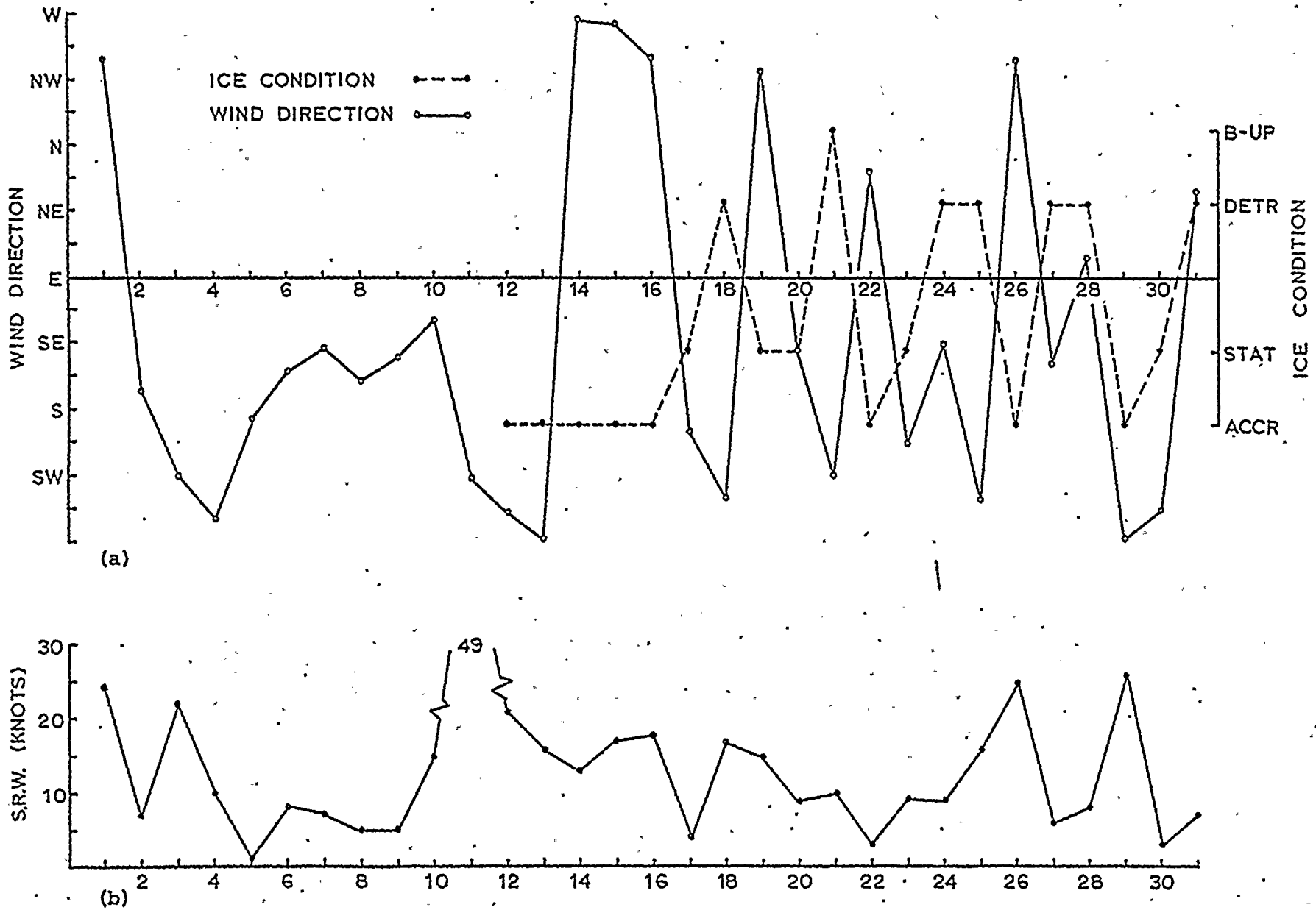

FIG. 7. Daily ice conditions vs. direction and speed of resultant wind: January 1975

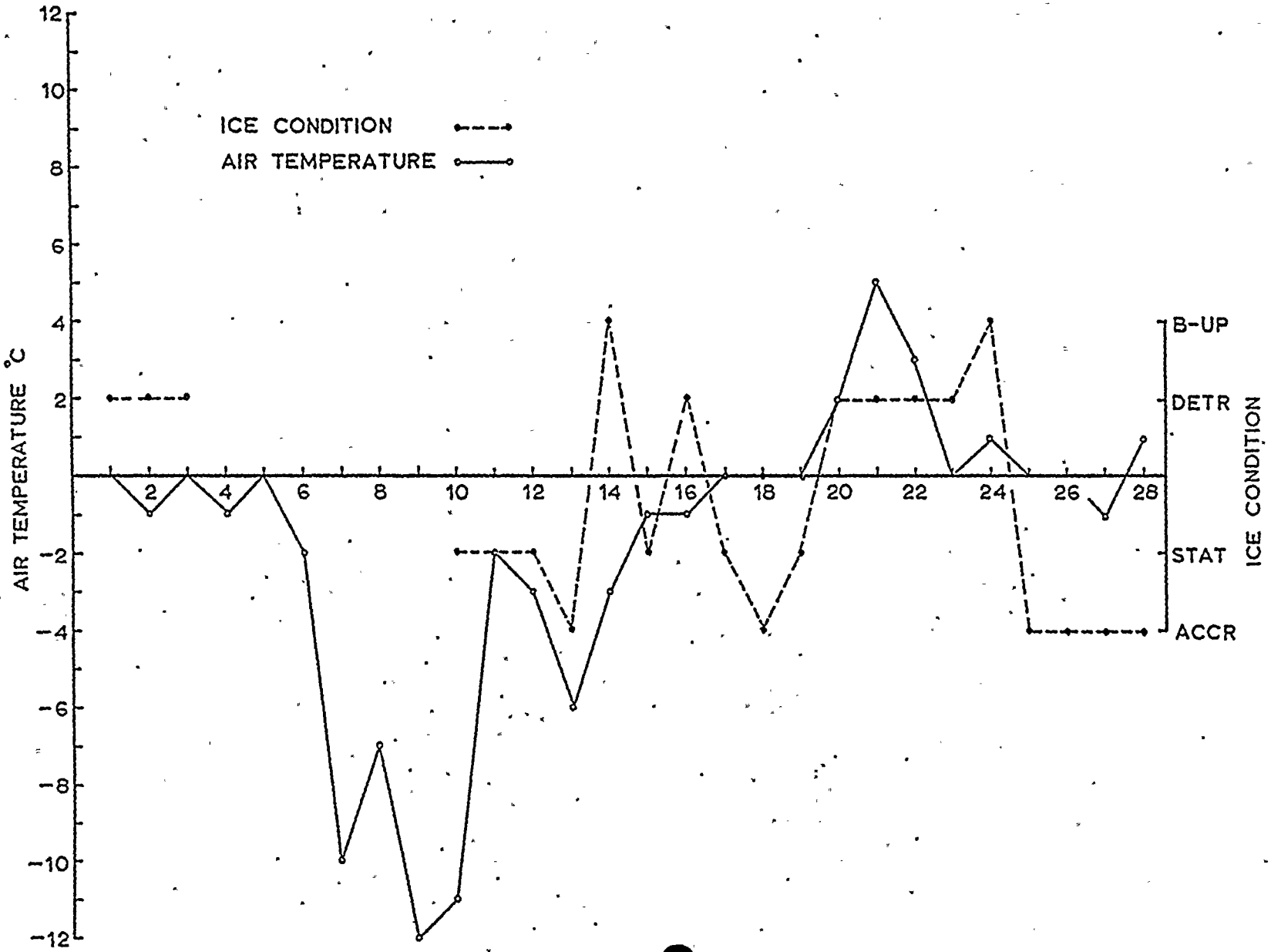

FIG. 8. Daily mean air temperature and ice conditions: February 1975

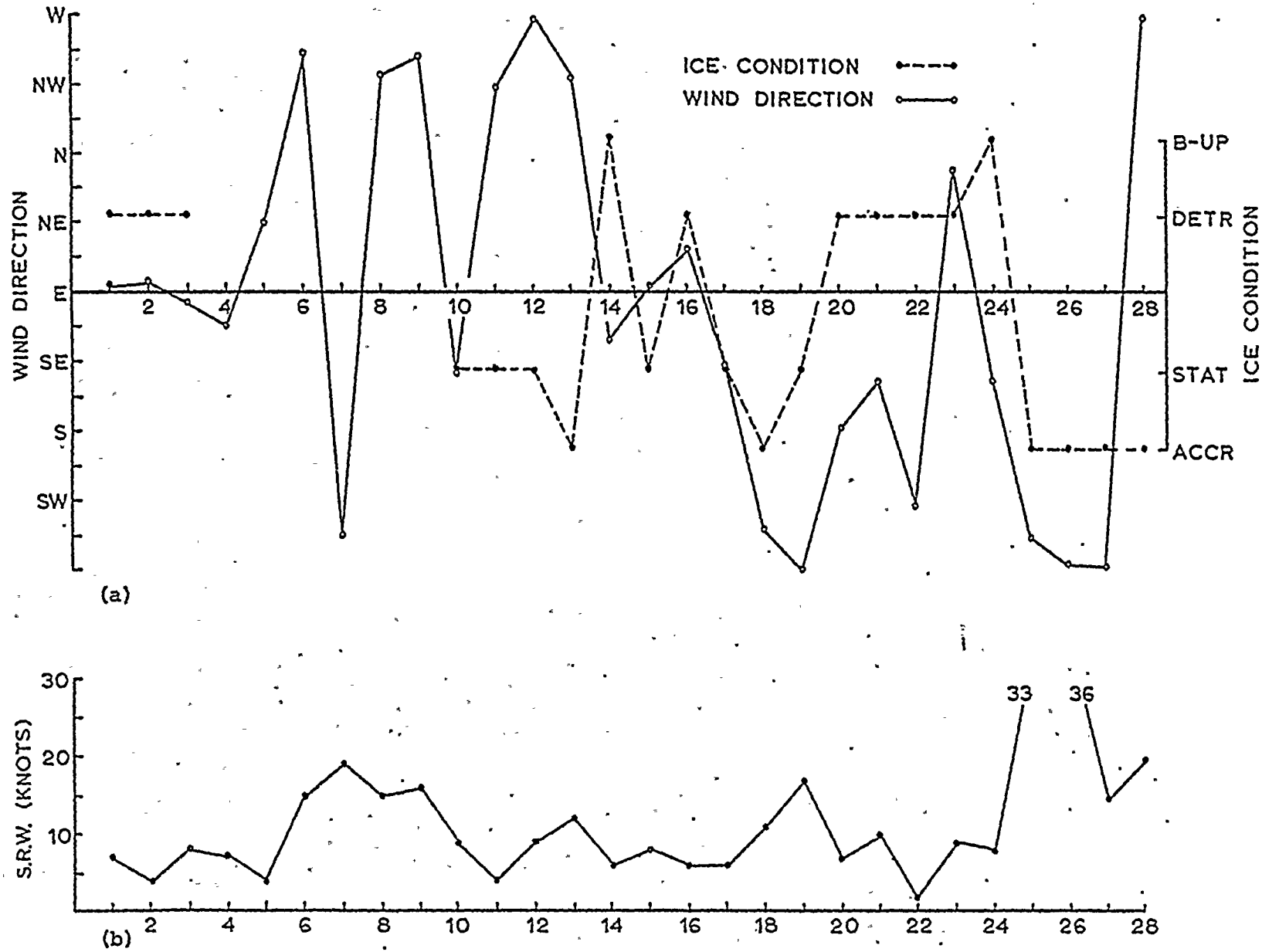

FIG. 9. Daily ice conditions vs. direction and speed of resultant wind: February 1975.

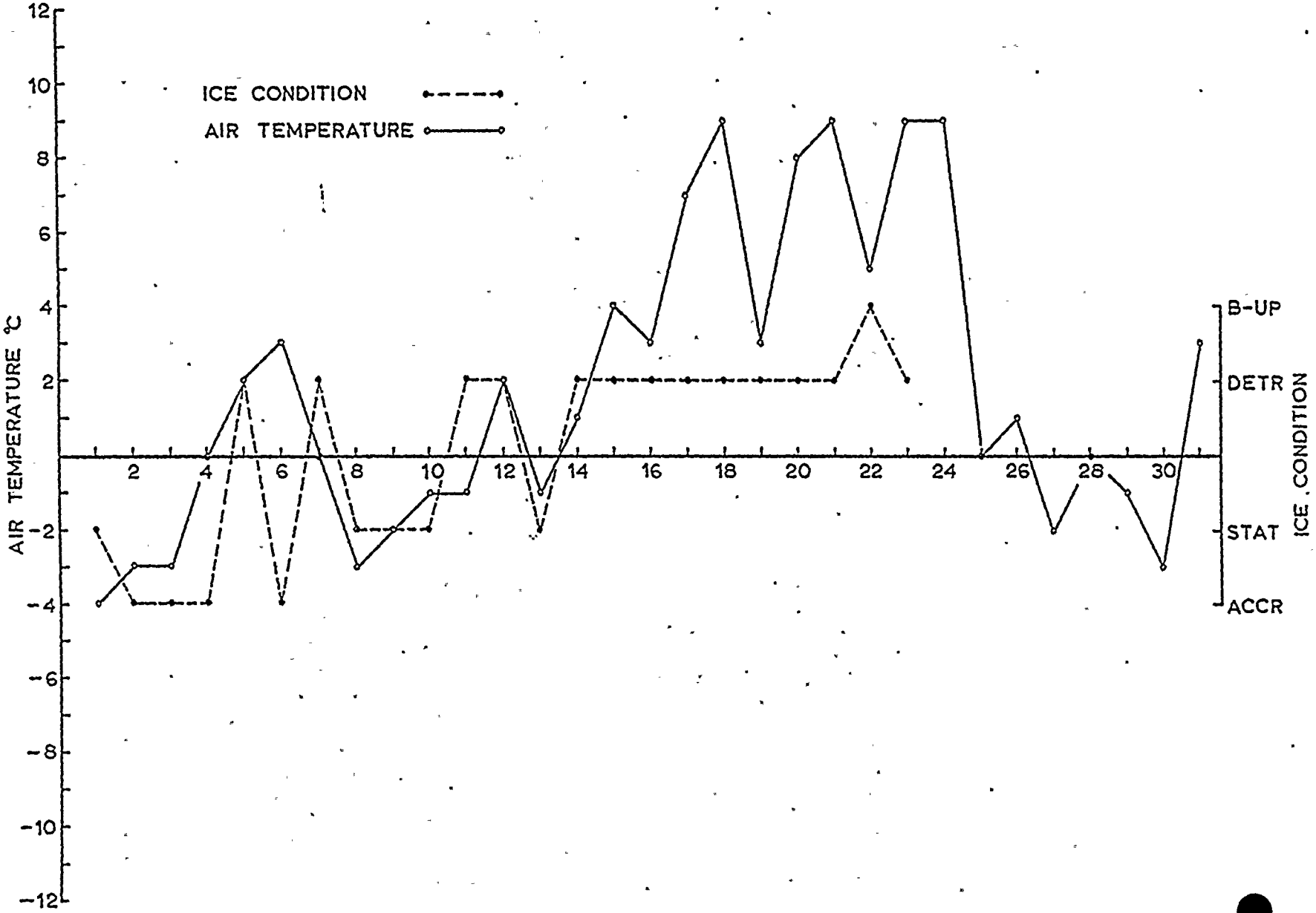

FIG. 10. Daily mean air temperature and ice conditions: March 1975

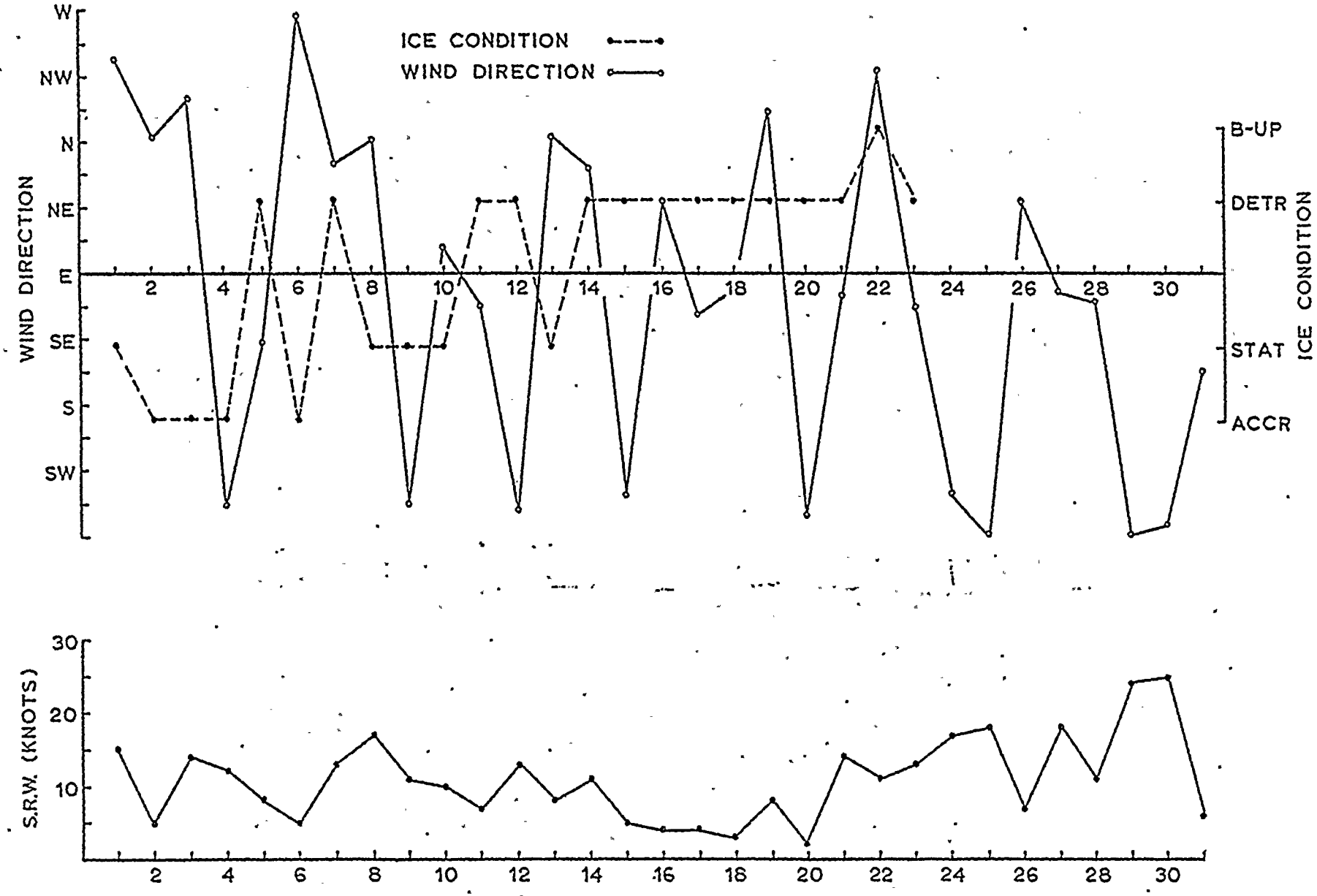

FIG. 11. Daily ice conditions vs. direction and speed of the resultant wind: March 1975

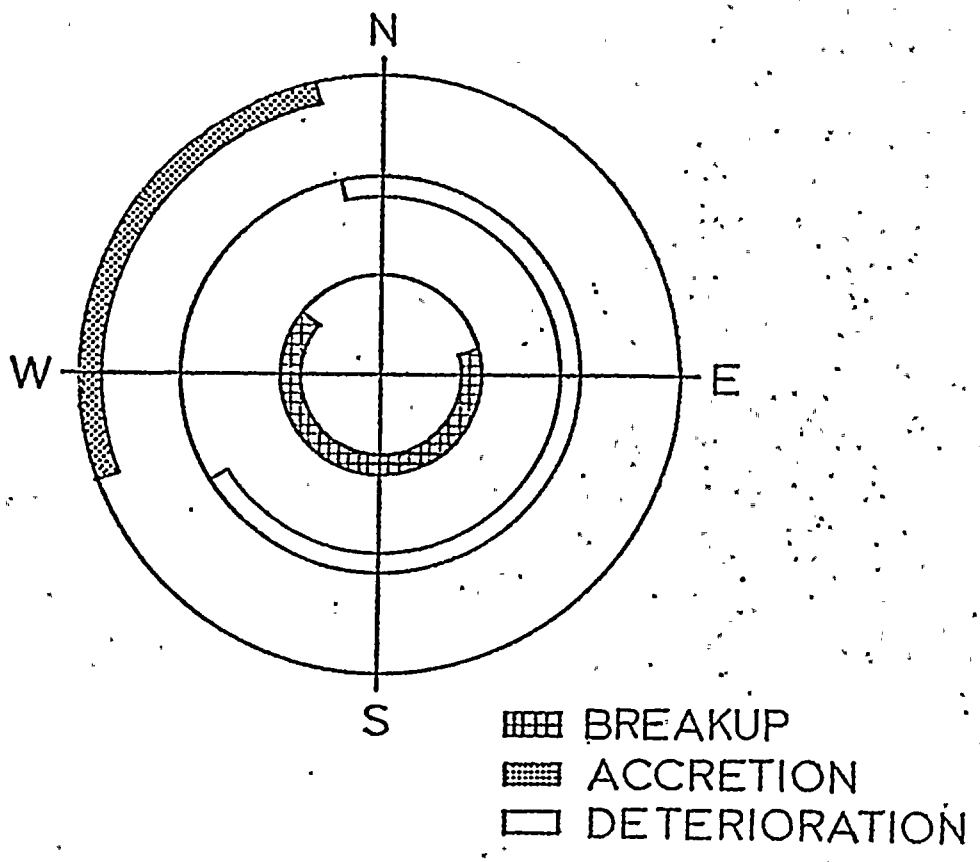

FIG. 12. Daily resultant wind direction vs. ice condition: January, February, and March 1975 for winds with persistence of 75% or greater.

presented in the graphical format.

Ice first formed at the study site on 12 January 1975 following an extreme drop in air temperature accompanied by onshore winds as indicated in Figures 6 and 7. These are prime conditions for lake ice accretion at this location on Lake Michigan. Subfreezing air temperatures and continued onshore winds resulted in further accretion for several days following the initial appearance of ice. This combination of conditions repeatedly produced the same results during the 1975 ice season as is evident in Figures 6 through 11.

Due to equipment malfunction, the photographic record is incomplete from 4 February to 9 February 1975. During this period there was significant ice accretion which resulted in the formation of two new ice ridges. The conditions during this period parallel closely those which promoted the initial ice formation in early January. The lowest air temperatures during the month of February occurred during this period. As might have been predicted, onshore winds of sufficient magnitude to produce moderate wave activity coupled with the subzero air temperatures promoted ice accretion. Onshore northwesterly winds and subzero air temperatures on 13 February again resulted in accretion immediately followed by breakup on 14 February as air temperatures rose and winds shifted to an offshore orientation.

Throughout January, February, and the first part of March, onshore winds and low air temperatures resulted in ice accretion. The data plotted on Figures 10 and 11 for 9 March 1975 appear contrary to the model sequence. Subfreezing air temperatures and onshore winds did not produce

additional ice accretion. During the night a wide zone of brash ice accumulated lakeward of the second ice ridge to a position past the third breaker zone. The winds changed from a northerly to a more westerly direction between 8 February and 9 February producing the brash ice accumulation as might be expected. However, during the daylight hours the extreme width of the brash ice zone shielded the ice complex from further ice ridge formation by preventing breaker formation.

The model stages of ice formation at the study site are most dependent upon the wind direction and speed. The dependence of ice condition on wind direction is summarized in Figure 12 . This figure was derived using composite wind data for January, February, and March 1975. Resultant wind directions for winds with a persistence of 75% or greater were plotted with the corresponding ice condition for each day. Winds of lesser persistence produced similar results. The static condition was represented by scattered points covering the entire 360 degrees and hence was not plotted. Static conditions were usually accompanied by variable winds of low speed having little effect on the ice complex.

Figure 12 shows no overlap between the accretion and deterioration stages unlike that between breakup and deterioration. Frequently deterioration is the precursor to the breakup stage. Simple deterioration of the ice complex by minor wave activity and above freezing air temperatures may pass into the breakup stage with an increase in wind speed or direction and subsequent escalation in wave activity.

Accretion and breakup may display a similar relationship. High onshore wind speeds may breakup the existing ice complex and relocate the

resulting ice blocks and fragments further inshore. The remnant ice fragments may be piled into an ice ridge-like structure not necessarily positioned over an offshore bar, but grounded at a location in equilibrium with the existant wave climate. When this equilibrium has been established, subsequent additions of freezing spray and wave-tossed brash ice will initiate the accretive stage with no change in wind direction thus offering one possible explanation for overlap between accretion and breakup in Figure 12 , The sequence of events recorded by the time-lapse system on 20 and 21 January 1975 document this process.

REFERENCES

Bryan, L.M. and M.G. Marcus. 1972. Physical characteristics of near-shore ice ridges. Arctic 25: (3)182-192.

Davis, R.A. Jr. and D.F.R. McGrary. 1965. Stability in nearshore bottom topography and sediment distribution, S.E. Lake Michigan: in Conf. on Great Lakes Research, 8th, Ann Arbor, 1965, Proc., U of M, GLRD Publ. 13, 222-231.

Maresca, J.W. Jr. 1975. Bluffline recession, beach change, and nearshore change related to storm passages along southeastern Lake Michigan. Ph.D. Dissertation, Univ. Michigan, Ann Arbor. 481 p.

O'Hara, N.W: and J.C. Ayers. 1972. Stages of shore ice development. Proc. 15th Conf. Great Lakes Res., Internat. Assoc. Great Lakes Res. p. 521-535.

Olson, C. 1973. Class notes from Natural Resources 442, Univ. Michigan, Ann Arbor.

Seibel, E., C.T. Carlson, and J.W. Maresca Jr. 1975. Lake and shore ice conditions on southeastern Lake Michigan in the vicinity of the Donald C. Cook nuclear plant: winter 1973-74, U of M, GLRD Publ. 55.

APPENDIX A. DAILY ICE CONDITIONS

12 January 1975	The last slide taken on this date shows the initial formation of an icefoot, the first evidence of lake ice in 1975
13 January 1975	Overnight ice accretion resulted in the formation of a fully formed icefoot, the first ice lagoon, and first ice ridge. Freezing spray and wave-tossed brash ice augmented the first ice ridge producing a hummocky appearance. Throughout the day a zone of unconsolidated floating ice fragments remained bounded by the first ice ridge and the second breaker zone.
14 January 1975	Slides depicting ice conditions on this date showed little visible change in the ice conditions.
15 January 1975	The second ice lagoon and the second ice ridge were formed overnight. Sediment darkened blowhole cones were formed by wave activity along the second ice ridge while wave-tossed ice fragments and freezing spray accumulated on its crest.
16 January 1975	Further addition of ice fragments and freezing spray increased the height of the second ice ridge until its height surpassed that of its more shoreward counterpart.
17 January 1975	Incomplete overnight formation of the third ice lagoon resulted in its termination shoreward of the third breaker zone.
18 January 1975	Wave activity broke up and dispersed the third ice lagoon. Waves breaking against the second ice ridge in the presence of remnant lagoonal ice fragments rejuvenated the ridge with freezing spray and wave tossed ice fragments.
19 January 1975	Prolonged wave activity eroded the second ice ridge decreasing its overall height.
20 January 1975	Wave activity during the night breached the second ice ridge and removed portions of the second ice lagoon.

21 January 1975	Continued wave decay reduced portions of the second ice ridge to grounded blocks and decomposed the second ice lagoon into floating brash ice.
22 January 1975	A zone of floating brash ice accumulated lakeward of the deteriorating second ice ridge. Snow and low wind speeds produced floating slush ice on the lake surface.
23 January 1975	Lakeward of the deteriorated second ice ridge brash ice accumulations consolidated in the absence of breaking waves.
24 January 1975	Brash ice concentrations lakeward of the stationary ice complex were dispersed by offshore winds. Scattered accumulations of floating brash ice were observed lakeward near the horizon in all photos taken on this date.
25 January 1975	Wave conditions intensified and broke up the deteriorated second ice ridge by late afternoon. Subsequently, the first ice ridge was visibly eroded although its height above the mean still water level was increased by the addition of freezing spray and wave-tossed ice fragments.
26 January 1975	The persistant high energy wave climate broke up the first ice ridge and forced the remnant ice blocks and ice fragments shoreward where they regrounded at a location near the plunge zone.
27 January 1975	Ice accretion was evident along the lakeward edge of the ice which had grounded the previous day. Zones of floating brash ice were visible on the lake surface in each slide taken on this date.
28 January 1975	There was no major change in the ice structures on this date.
29 January 1975	Significant overnight deterioration of the ice ridge was evident in the first photo taken on this date. Intensified wave activity accelerated deterioration of the ice ridge and produced several large blowhole cones.

30 January 1975	The narrow zone of open water located between the ice ridge and the shoreline was filled with wave-tossed ice during the night, otherwise there was no visible change in the ice conditions on this date.
31 January 1975	Cracks which developed along the lakeward edge of the ice complex were indicative of undercutting by waves. The unsupported portions of the ice complex subsequently collapsed.
1 February 1975	The ice complex was further deteriorated by overnight wave activity. However, little additional change was noted during the day.
2 February 1975	There was no major change in the ice conditions on this date.
3 February 1975	Only one slide was available to document ice conditions on 3 February. Wave activity during the night produced visible deterioration of the ice ridge.
4-9 February 1975	No photographs were available for this period.
10 February 1975	There was significant ice accretion during the interval of 4-9 February. The slides taken on 10 February show a large icefoot, the first and second ice lagoons and the first and second ice ridges. The lake was covered to the apparent horizon with patches of floating brash ice.
11 February 1975	Ice conditions were nearly identical with those of the previous day. Throughout the day the lake surface became more densely covered with floating ice fragments.
12 February 1975	Slides taken 12 February showed no visible change in the ice ridge system. However, slush ice was evident on the calm lake surface in the last slide taken on this date.
13 February 1975	Extensive nocturnal ice accretion was evident in the first photo taken 13 February. The icefoot and two ice ridges were visible shoreward of the new accumulation of floe ice.

14 February 1975	Early morning slides showed the lake to be ice covered to the apparent horizon. During the day a zone of open water formed lakeward of the second ice ridge as the floe ice moved offshore.
15 February 1975	A linear zone of floating brash ice remained stationary lakeward of the second ice ridge, beyond this the lake was free of ice.
16 February 1975	The brash ice located lakeward of the second ice ridge was dispersed during the day by offshore winds.
17 February 1975	There were no major changes in the ice conditions on this date.
18 February 1975	The stationary ice ridge complex remained unchanged although floating brash ice accumulated against the lakeward edge of the second ice ridge.
19 February 1975	The width of the floating brash ice accumulation lakeward of the ice ridge system fluctuated during the day, otherwise there was no major change in the ice conditions.
20 February 1975	The first photo on this date showed the third ice lagoon in the initial formative stages. By late morning, winds had broken up this ice lagoon and all photos taken after mid-day showed unconsolidated, floating brash ice covering the lake surface to the apparent horizon.
21 February 1975	The existing ice ridge system consisted of the ice-foot and the first and second ice lagoons and ice ridges showed little overall change. Extinct blowhole cones darkened as sun rot concentrated sedimentary lag deposits. Floating ice was visible near the apparent horizon.
22 February 1975	Above freezing air temperatures during the day resulted in further deterioration of the ice ridge complex. Floating ice fragments were visible lakeward of the second ice ridge.
23 February 1975	Minor deterioration produced little change in the ice conditions on 23 February.

24 February 1975	Approximately one-third of the second ice ridge visible in the camera's field of view was reduced to grounded ice blocks during the night. That portion of the second ice lagoon located shoreward of the breached ridge was totally removed by offshore winds. Later photos showed further break up of the second ice ridge and ice lagoon as well as portions of the first ice ridge.
25 February 1975	The first photo taken on 25 February showed grounded remnant ice blocks coincident with the second breaker zone. Wave activity eventually forced the ice blocks and other ice fragments shoreward grounding them near the plunge zone.
26 February 1975	Wave-tossed ice and freezing spray augmented the lakeward edge of the grounded ice mass.
27 February 1975	Erosion of the steep lakeward face of the ice by waves breaking in the absence of floating ice fragments was evident in the photos taken 27 February.
28 February 1975	Wave activity further deteriorated the ice mass throughout the day.
1 March 1975	Overnight breakup of the remaining ice rejuvenated the icefoot. Several large ice blocks were grounded along the icefoot at the waterline.
2 March 1975	Ice accretion during the day produced the first ice lagoon and first ice ridge. Floating brash ice was forced shoreward toward the accreting ice front by wind and wave activity.
3 March 1975	Ice accretion continued on this date forming the second ice lagoon and second ice ridge. By late afternoon, the third ice lagoon was in the initial stages of formation.
4 March 1975	Floating lake ice accumulated to a position near the apparent horizon.
5 March 1975	Offshore winds forced the floating pack ice lakeward opening a large zone of open water lakeward of the second ice ridge.

6 March 1975	During the night, brash ice accumulated along the lakeward edge of the second ice ridge. Floating ice fragments forced shoreward by onshore winds widened the zone of floating ice.
7 March 1975	Floating brash ice was dispersed overnight by offshore winds. Rejuvenation of the second ice ridge by freezing spray and wave-tossed slush ice was evident in the photos as winds rotated to an onshore quadrant.
8 March 1975	Nocturnal accretion along the second ice ridge filled locations of low relief and resulted in a more continuous, uniform ice ridge. Floating brash ice was located along the lakeward edge of the second ice ridge in each photo.
9 March 1975	The first photo taken on 9 March showed the zone of the floating brash ice lakeward of the second ice ridge had widened during the night. There was little change in the ice conditions during the day.
10 March 1975	Offshore winds forced all floating ice lakeward. The nearshore ice complex, complete to the second ice ridge, showed little change throughout the day.
11 March 1975	Pack ice was visible near the horizon only in the first photo taken on 11 March. Otherwise there was no apparent change in the ice conditions.
12 March 1975	Sun rot concentrated the sandy lag deposits overlying the nearshore ice complex.
13 March 1975	There was no major change in the ice conditions on this date. Lag deposits continued to concentrate further darkening of the ice surface.
14 March 1975	Above freezing air temperatures during the previous several days produced a narrow zone of open water along the shoreline, otherwise there was no major change in the ice conditions.
15 March 1975	The nearshore ice complex was slowly deteriorating due to above freezing air temperatures. Change was subtle and manifested in darkening coloration or the gradual

erosion of the lakeward edge of the second ice ridge by low energy wave activity.

16 March 1975 — The narrow band of open water located between the shoreline and the ice widened as the ice complex continued to deteriorate.

17 March 1975 — Further deterioration of the ice mass was accompanied by continued concentration of sedimentary lag deposits.

18 March 1975 — The second ice ridge was reduced to a series of connected extinct blowhole cones and the second ice lagoon deteriorated to floating ice fragments.

19 March 1975 — A series of isolated blocks surrounded by floating ice fragments marked the location of the second ice ridge.

20 March 1975 — Offshore winds removed remnant ice fragments of the second ice lagoon leaving only isolated ice blocks to mark the former position of the second ice ridge. Although still intact, the first ice ridge was isolated from the shore by a zone of open water.

21 March 1975 — Several remnant blocks of the second ice ridge were removed from the study site by offshore winds during the night. Numerous ice fragments from the deteriorating ice complex could be seen floating offshore.

22 March 1975 — The first ice ridge was breached in several locations by wave activity and the resulting ice fragments were washed onto the shore.

23 March 1975 — The ice blocks and fragments grounded along the waterline deteriorated throughout the day and only a few scattered blocks were visible in the last photo taken on 23 March.

24 March 1975 — No ice was visible at the study site.

Terminology Used in Slide Description

ACCRETION: A visible lakeward advance of the ice front.

DETERIORATION: A gradual decay of the nearshore ice complex apparent only after viewing several slides in sequence.

BREAKUP: A rapid decay and dispersal of the nearshore ice usually taking place in the period of a few hours.

ICEFOOT: A small ridge-like ice structure which forms at the waterline.

ICE LAGOON: A tabular ice formation which shows little vertical relief and is confined between the icefoot and first ice ridge or between two ice ridges.

ICE RIDGE: A linear ice structure having variable vertical relief and usually aligned parallel with the shoreline. A cross-sectional view would show a nearly vertical lakeward face and more gently sloping landward face.

FAST ICE: An ice formation which has greater thickness than an ice lagoon and which extends from the icefoot nearly to the location of the first offshore bar.

SHORE ICE: An ice mass which has been deposited on the beach and is terminated near the waterline.

BRASH ICE: Floating, unconsolidated ice fragments usually formed offshore or produced by the break-up of an ice system.

SLUSH ICE: A floating, unconsolidated ice-water mixture often produced on the lake surface during snowfalls.

APPENDIX B. GRAPHICAL TECHNIQUES FOR DETERMINATION OF MONITORED VARIABLE LOCATIONS

The discussion which follows describes the methods used in determining the distance from the baseline to each monitored variable. Figure is used as the basis for reference in the discussion.

1. The ground coordinate points and regression lines are plotted on the grid by the computer's digital plotter. The location of each monitored variable is defined by a unique linear array of plotted characters:

(⊹) = baseline (Line A)

(⊡) = waterline (Line B)

(△) = ice ridge (Line C)

(+) = breaker zone (Line D)

2. Construct the normal to the baseline (Line A) at point (F).

3. Point (G) is formed by the intersection of the baseline normal and line (E) which marks the location of the breaker zone. Line (GH) is constructed parallel to the ordinate and of sufficient length to intersect a line parallel to the abscissa through point (F).

4. After measuring the length of lines (FH) and (GH), application of the proper plotting scale and the Pythagorean Theorem will yield the perpendicular distance from the baseline to this breaker zone. This technique is repeated for each monitored variable, at three positions along the baseline, the mean of the three values for each variable is retained.

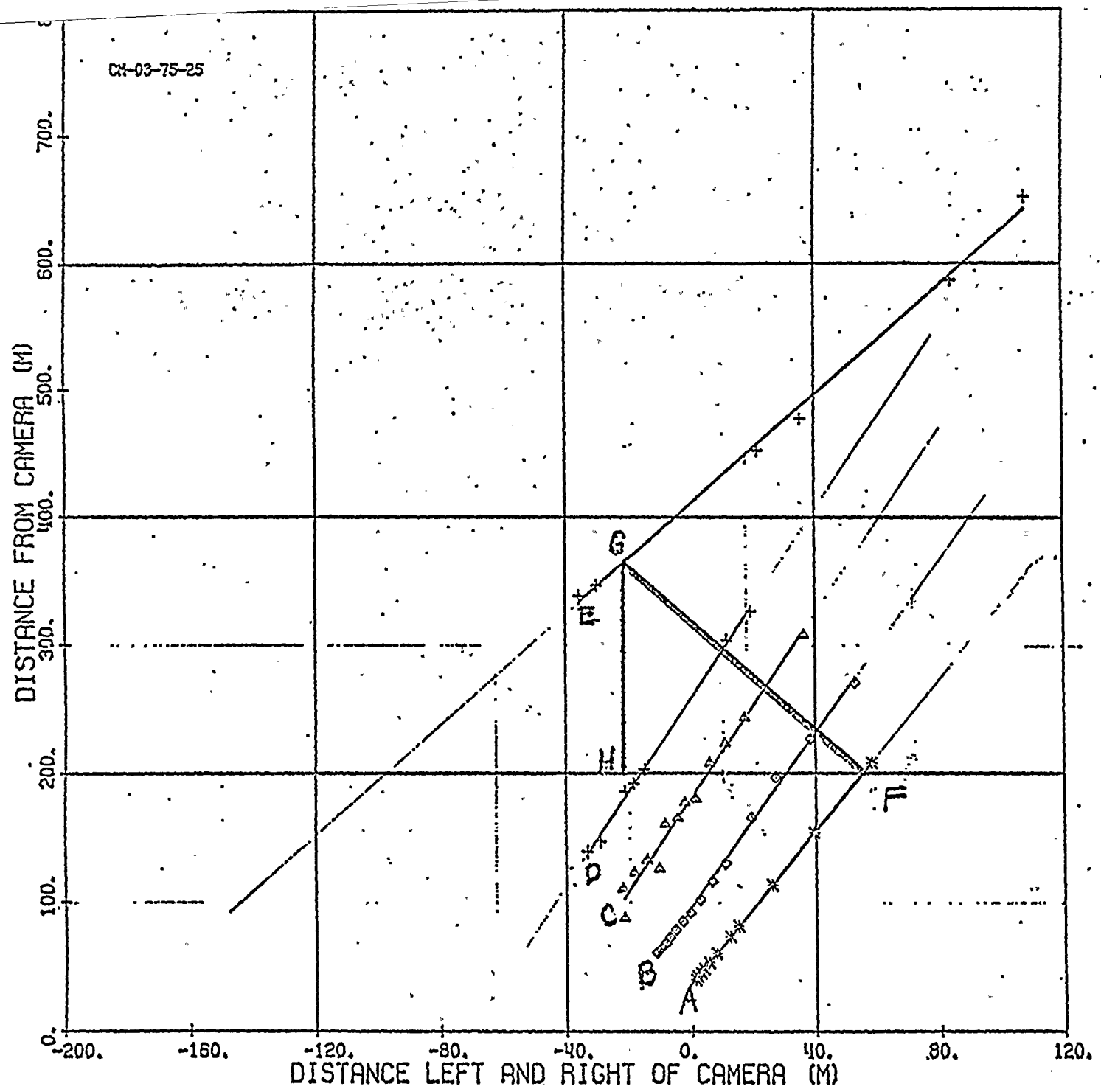
CH-03-75-25
DISTANCE FROM CAMERA (M)
0.
100.
200.
300.
400.
500.
600.
700.
-200.
-160.
-120.
-80.
-40.
0.
40.
80.
120.
DISTANCE LEFT AND RIGHT OF CAMERA (M)
G
H
E
F
D
C
B
A

APPENDIX C. SOURCES OF POSSIBLE ERROR IN THE PHOTOGRAPHIC ANALYSIS

We utilized a high oblique photographic method to monitor the ice conditions along the shoreline of Lake Michigan. This method, like most, has limitations on the accuracy of the numbers one obtains. This appendix describes and, where possible, quantifies errors that were encountered in the analysis. The errors recognized and discussed independently below are: slide remounting; marking points on the oblique representation; computer plotting; linear approximation to monitored variable locations; graphical analysis of computer plots; and obscured apparent horizon.

SLIDE REMOUNTING

For analysis each slide was removed from the original cardboard mount and was remounted on a 2 inch plexiglass square. Alignment of the sprocket holes in the color transparency with the guide lines on the plexiglass mount was only as accurate as the analyst's eye. Alignment with a given guide line was accurate within the width of that guide line (0.001"); hence, this source of error was negligible.

The overall position of the color transparency on the plastic mount was also checked. Before the oblique coordinates were assigned to data points on the projected image, the position of the photograph's projected principal point was verified. If the color transparency had been aligned either too high or too low on the plastic mount, the position of the principal point was corrected. Typical values for principal point displacement ranged from 0.10" to 0.20" in the projected image.

In order to evaluate the possible error in computed ground coordinates resulting from a displaced principal point, one slide was analyzed twice. The data for the slide were run first without the position of the principal point corrected and subsequently with the position correction. The results of the comparison indicated that the small errors in principal point location encountered in the study produced differences in the computed ground coordinates not exceeding 0.03m.

MARKING POINTS ON THE OBLIQUE REPRESENTATION

The method of single image photographic analysis employed in this study requires that all data points selected for ground coordinate calculations be located a known elevation above the datum. In cases where a variable's height above the MSWL datum was unknown, accurate determination of its ground coordinates required that its position in the oblique representation be marked where its intersection with the water surface was evident. Due to the small camera depression angle, data points marked on the oblique image at some unknown elevation would introduce large displacement errors.

To minimize displacement errors, data points were selected at the datum plane or their elevation above the MSWL datum was determined prior to the ground coordinate calculations. Surveyed elevations were used for control points and the height of the ice ridges above the datum was evaluated using computer program HEIGHT.

COMPUTER PLOTTING

The computer-generated graphical output was produced by a CALCOMP 780/763 digital plotter. Due to the orientation of the monitored variables in the oblique photographs the ground coordinates and regression lines were plotted on a cartesian coordinate grid scaled 1 inch : 40 meters along the abscissa and 1 inch : 100 meters along the ordinate.

The plotting pen moves in incremental steps of varying length dependent upon the mode and step-size selected by the Michigan Terminal System (MTS) CALCOMP post-processor. INCREMENTAL mode controls pen movement with step-size of either 0.005 or 0.0025 inch per command in the horizontal or vertical directions. Step-size may be increased to 0.0185 inch per command in 0.00125 inch steps in the ZIP mode. The coordinate system used in this study restricted the maximum plotting error to less than 0.2 meters along the abscissa and 0.5 meters along the ordinate. Overall plotting error should be considerably less than these maximum values since the MTS post processor selects the most appropriate step-size in order to maximize plotting speed and accuracy.

LINEAR APPROXIMATION TO MONITORED VARIABLE LOCATIONS

The subroutine REGRES in the computer program ICE75 performs a linear regression analysis on the real ground coordinates supplied to it by the subroutine PHOTO. Subroutine REGRES determines the equation of the best fit line to each linear array of coordinate points defining the location of a unique variable in the real ground coordinate system. The tabular output for each plotted variable includes a regression table summarizing the statistical parameters associated with the regression analysis. The linear correlation coefficients for the plotted variables monitored in this study were greater than 0.98 justifying the linear approximation to their actual location. In order of higher degree of linear correlations were, respectively, breaker zones, the ice ridges, the waterline, and the baseline.

The coordinate points locating the position of the ice ridges and breaker zones displayed the most scatter about their respective regression lines. This scatter may be attributed to two sources; human error in marking the data points in the oblique representation and the natural variability in the location of the monitored variable. The breaker zones (offshore bars) have a natural width and may be defined by several waves breaking at

a given instant in close proximity to one another, but not along a perfectly straight line. The ice ridges have an irregular lakeward edge due to their mode of formation and constant exposure to wave activity. This natural irregularity results in some scatter of the selected data points.

GRAPHICAL ANALYSIS OF COMPUTER PLOTS

A detailed description of graphical techniques used in this analysis may be found in Appendix C. All distances to monitored variable locations were measured perpendicular to the baseline using a dial caliper accurate to 0.001 inch. The cartesian ground coordinate grid used in this study was scaled 1 inch : 40 meters along the abscissa and 1 inch : 100 meters along the ordinate. This selection of plotting scale restricted measurement errors to 0.04 meters and 0.10 meters in the x and y directions, respectively.

ERROR RESULTING FROM AN OBSCURED HORIZON

For the analysis of the single-image high oblique photographs it was necessary to determine the distance between the principal point and the apparent horizon in the projected oblique image. This distance was subsequently used to define the geometry of the principal plane diagram. Since the equivalent vertical photograph coordinates are based on this geometry, error may be introduced by an obscured horizon.

Although the correct location of an obscured horizon may be determined by several analytical techniques, none were needed for this study. A large selection of photographs provided many with clear apparent horizons enabling the analyst to completely avoid this potential problem.

APPENDIX D. SUMMARY TABLE OF CLIMATIC VARIABLES: JANUARY, FEBRUARY, MARCH 1975

January 1975

Date	Wind direction 0700	1000	1300	1600	PHI	Wind speed (knots) 0700	1000	1300	1600	SRW
1	WNW	WNW	WNW	NW	153	22	25	30	22	24
2	SSE	SSE	S	S	-176	10	8	6	4	7
3	SW	SW	SW	SW	-135	25	12	25	25	22
4	WNW	W	SW	SW	-163	11	12	15	7	10
5	WNW	SSW	SE	ESE	- 96	10	3	6	6	1
6	ESE	ESE	SE	SW	- 64	15	11	5	20	8
7	SE	SE	SSW	E	- 49	12	10	6	5	7
8	N	SW	NNW	E	- 70	15	14	13	7	5
9	WSW	WSW	SE	ESE	- 54	3	5	10	12	5
10	ESE	ESE	ESE	SE	- 29	16	14	15	17	15
11	SW	SW	SW	SW	-135	50	50	50	45	49
12	WSW	WSW	WSW	WSW	-158	25	23	20	18	21
13	W	W	WSW	W	-175	20	15	15	15	16
14	WNW	W	W	W	175	12	15	15	13	13
15	W	WNW	WNW	WSW	174	20	21	15	17	17
16	NNW	WNW	WNW	WNW	151	12	20	21	20	18
17	W	SE	SE	SSE	-105	16	6	7	7	4
18	SSW	SW	WSW	WSW	-149	8	12	23	29	17
19	WNW	NW	NW	NW	142	18	10	10	22	15
20	ESE	SE	SSE	S	- 52	10	14	7	8	9
21	SSE	SSW	WSW	WSW	-135	11	7	18	15	10
22	NNE	ENE	E	W	72	10	4	4	8	3
23	SW	SSW	SSW	S	-113	10	9	8	9	9
24	SE	SE	SE	SE	- 45	7	10	10	10	9
25	SE	WSW	WSW	WSW	-152	7	17	20	30	16
26	WNW	WNW	NW	NW	148	32	25	24	20	25
27	WNW	SE	SSE	SE	- 59	5	10	9	8	6
28	*	NE	E	E	13	*	8	10	8	8
29	SW	W	W	WNW	-178	20	28	35	28	26
30	WNW	SSW	WSW	WSW	-158	4	4	4	3	3
31	NNW	NE	E	ENE	59	15	10	8	5	7

* No data available

February 1975

Date	Wind direction 0700	1000	1300	1600	PHI	Wind speed (knots) 0700	1000	1300	1600	SRW
1	E	E	E	ENE	4	5	8	9	5	7
2	SE	E	ENE	NNE	6	6	5	3	5	4
3	E	E	ESE	NNE	- 7	7	7	10	8	8
4	ESE	ESE	ESE	ESE	- 23	7	7	8	8	7
5	ENE	ENE	NE	NNW	45	5	5	4	4	4
6	E	WNW	WNW	WNW	156	4	20	20	25	15
7	WSW	WSW	WSW	WSW	-158	17	20	25	15	19
8	WNW	NW	NNW	WNW	142	18	17	13	15	15
9	NW	NW	W	WNW	154	15	15	19	19	16
10	*	SE	SE	SSE	- 53	*	10	7	10	9
11	WNW	NW	NE	WNW	134	10	4	5	2	4
12	E	NW	W	W	178	4	2	20	20	9
13	NNW	NW	WNW	WNW	140	15	10	15	10	12
14	SE	SE	ESE	ESE	- 31	4	5	7	8	6
15	E	E	E	ENE	3	10	9	10	5	8
16	NE	ENE	ENE	ENE	27	5	5	8	8	6
17	E	ESE	SSW	SSW	- 48	10	14	10	5	6
18	WSW	SSW	SW	W	-153	20	5	10	10	11
19	WNW	W	WSW	W	-179	15	20	18	19	17
20	SSE	SSW	SE	SW	- 88	10	7	10	10	7
21	SE	SE	SSE	SSE	- 58	7	10	10	15	10
22	SW	SW	SSW	NNE	-137	5	5	3	4	2
23	NNW	NNE	NNE	NNE	79	10	12	8	9	9
24	*	ESE	SSE	SSE	- 57	*	6	10	8	8
25	SW	WSW	W	WSW	-159	29	36	35	35	33
26	W	W	W	WSW	-175	35	39	38	33	36
27	WNW	W	WSW	SW	-176	22	19	15	10	15
28	WSW	WSW	WNW	WNW	180	20	25	25	22	21

* No data available

March 1975

Date	Wind direction 0700	1000	1300	1600	PHI	Wind speed (knots) 0700	1000	1300	1600	SRW
1	WNW	NW	WNW	NW	146	15	15	15	17	15
2	NE	NW	*	*	94	6	7	20	10	5
3	NNW	NNW	NW	NNW	120	15	10	18	12	14
4	WSW	WSW	WSW	WSW	-158	15	10	12	12	12
5	ESE	SE	SE	SSE	- 48	5	10	10	9	8
6	NW	WSW	W	WNW	177	5	9	6	3	5
7	NE	NNE	N	N	76	8	18	20	9	13
8	NNW	NNE	N	N	92	20	15	18	18	17
9	WSW	WSW	WSW	WSW	-158	12	13	13	8	11
10	E	ENE	ENE	ENE	18	8	12	12	9	10
11	ENE	SE	ESE	ESE	- 21	4	5	10	10	7
12	SSE	SW	W	W	-162	5	16	20	20	13
13	W	NE	NNE	NNW	94	15	15	15	10	8
14	NE	NE	N	NNW	73	12	10	19	7	11
15	W	S	WSW	WSW	-151	6	5	8	5	5
16	SE	ESE	N	NNE	50	5	4	10	8	4
17	E	SE	S	N	- 28	6	10	7	7	4
18	ESE	SE	WNW	N	- 9	10	8	5	6	3
19	N	NW	NNW	NNW	112	5	4	11	12	8
20	ESE	SW	NW	WNW	-166	9	7	7	5	2
21	ESE	ESE	ESE	E	- 15	10	15	12	20	14
22	NNW	NW	WNW	WNW	138	10	20	12	5	11
23	*	ESE	ESE	ESE	- 23	*	12	10	17	13
24	ESE	WSW	WSW	WSW	-150	12	18	26	30	17
25	WSW	WSW	NW	NW	-178	35	22	18	10	18
26	ENE	ENE	NNW	NE	50	8	10	10	8	7
27	ESE	E	ESE	E	- 11	15	22	20	18	18
28	E	ESE	ESE	ESE	-.17	12	10	14	10	11
29	WNW	WSW	WNW	WSW	-179	22	25	28	28	24
30	W	W	WSW	W	-174	23	22	27	30	25
31	SE	SE	SSW	SSW	- 67	8	11	5	5	6

* No data available

	January 1975			February 1975			March 1975		
Date	Mean Air Temp °C	Mean Water Temp °C	Ice Cond.	Mean Air Temp °C	Mean Water Temp °C	Ice Cond.	Mean Air Temp °C	Mean Water Temp °C	Ice Cond.
1	- 2	2	NONE	0	1	DETR	- 4	1	STAT
2	- 2	2	NONE	- 1	2	DETR	- 3	1	ACCR
3	1	2	NONE	0	2	DETR	- 3	1	ACCR
4	1	2	NONE	- 1	2	*	0	1	ACCR
5	0	2	NONE	0	2	*	2	1	DETR
6	0	1	NONE	- 2	2	*	3	1	ACCR
7	4	1	NONE	-10	1	*	0	1	DETR
8	7	2	NONE	- 7	1	*	- 3	1	STAT
9	2	2	NONE	-12	1	*	- 2	1	STAT
10	9	2	NONE	-11	1	STAT	- 1	1	STAT
11	- 2	2	NONE	- 2	0	STAT	- 1	1	DETR
12	-10	2	ACCR	- 3	1	STAT	2	1	DETR
13	-11	1	ACCR	- 6	1	ACCR	- 1	2	STAT
14	-10	1	ACCR	- 3	1	B-UP	1	1	DETR
15	- 4	1	ACCR	- 1	1	STAT	4	1	DETR
16	- 4	1	ACCR	- 1	2	DETR	3	1	DETR
17	- 3	1	STAT	0	1	STAT	7	1	DETR
18	0	1	DETR	0	1	ACCR	9	2	DETR
19	- 2	1	STAT	0	1	STAT	3	2	DETR
20	- 9	1	STAT	2	1	DETR	8	2	DETR
21	- 1	1	B-UP	5	1	DETR	9	2	DETR
22	- 2	1	ACCR	3	1	DETR	5	2	B-UP
23	- 1	1	STAT	0	1	DETR	9	2	DETR
24	1	1	DETR	1	1	B-UP	9	2	NONE
25	2	1	DETR	0	1	ACCR	0	2	NONE
26	- 3	1	ACCR	0	1	ACCR	1	2	NONE
27	- 2	1	DETR	- 1	1	ACCR	- 2	3	NONE
28	2	1	DETR	1	1	ACCR	0	3	NONE
29	2	1	ACCR				- 1	3	NONE
30	- 1	1	STAT				- 3	3	NONE
31	2	1	DETR				3	3	NONE

* No data available

PRELIMINARY EVALUATION OF THE EFFECT OF COOK PLANT'S THERMAL DISCHARGE ON SHORE ICE AT THE PLANT SITE

The winter of 1975-76 was exceptionally mild. The pertinent photographs of that winter have been measured and analysed and the ice-condition graphs are included in the other submittals. They show nothing different from what has previously been reported by Seibel, Carlson, and Maresca (1975).

During the ice period of the winter of 1974-75 the plant was in the power ascention and testing phase and no meaningful information on the effect of the thermal discharge on ice was obtained.

Prior to the winter of 1976-77 the camera-monitor system was converted to a stereo-photograph system, with a second identical camera matched to the first through an improved timing unit and mounted on an adjacent window frame of the plant personnel office. The stereo-pairs of photographs from this camera system have been previewed and are undergoing measurement prior to submittal to computer analysis. Since the winter of 1976-77 was the first during which Cook Plant unit 1 was in operation and could have produced a melt-hole in the ice along shore, a program of daily photographs by hand-held camera of the north discharge area was instituted through a west-looking window of the plant, also.

The winter of 1976-77 was unusually severe, and fog, snow, and ice on the windows through which photos were being taken resulted in some lost data. The greatest loss, however, was due to the plant's shutdown for refueling at at the very peak of the coldest weather.

As the plant came back on line we coordinated carefully with plant personnel and made an aerial overflight of Cook Plant and the other plants on southeastern Lake Michigan as a warming trend was beginning to develop but before serious deterioration in the ice complex had begun.

The overflight took place on 2 March 1977. The ice-field of southeastern Lake Michigan on this day was the heaviest we have yet observed. Numerous pressure-ridges and much clear blue ice, both rare in our previous experience, were present and indicative of the severity of the winter. Figure 1 shows the melt-hole at Cook Plant on 2 March. On that day the melt-hole not at full size, even for unit 1, for the plant was back to only 48% of full power after refueling.

For the photograph the plane was put into a vertical bank almost over the melt-hole. This particular photograph was chosen because it shows the full extent of the melt-hole and the Cook Plant primary buildings. The largest of the plant buildings is the two-unit turbine building; without a small attached service building at the north (left) end, this building is 712 feet long parallel to shore. Scaling from the length of the turbine building in the photograph (with some liberality for the obliquity of the photograph) the melt-hole was approximatley 2100 feet long from north to south and 1800 feet from east to west. The hole lies lakeward of the outer ice ridge, and in the photograph has apparently not weakened that ridge. The melting appears to be directed lakeward as evidenced by the loose ice cakes at the bottom of the photograph.

On 16 March, after the plant was up to 91% of full power, we again overflew the southeastern shore of the lake. At this time the spring melt-off was in progress, and its effect plus that of Cook Plant at nearly full power should have produced maximum damage to the shore ice complex. Figure 2 is a view from west to east showing the plant and the associated shore ice; in the foreground is the fan-shaped whitish discharge plume of the plant directed to the left (north) and offshore. In front of the plant the ice structure is somewhat deteriorated, but in Figure 3 in the increasing

distance, similar deteriorations of the ice structure well away from the plant's discharge are present before the ice structure disappears in the general spring melt-off in the far distance.

The plant's history of generation from refueling until 16 March is given in the following table.

Date		Percent of full power
23 February		8
24		25
25		5
26		27
27		35
28		47
1 March		47
2	Overflight	48
3		57
4		66
5		69
6		69
7		69
8		74
9		82
10		43
11		21
12		74
13		89
14		89
15		90
16	Overflight	91

REFERENCE

Seibel, E., C. Carlson, and J. Maresca Jr. 1975. Lake and shore ice conditions on southeastern Lake Michigan in the vicinity of the Donald C. Cook Nuclear Plant: winter 1973-74. Spec. Rep. 55, Great Lakes Res. Div., Univ. of Michigan, Ann Arbor, Mich. 62 p.

FIG. 1. Melt-hole of Cook Plant unit 1 on 2 March 1977. Ice ridges parallel to shore appear undamaged. Discharge water melting into heavy sheet ice in foreground. Plant at 48% of full power; see table for previous days' power levels.

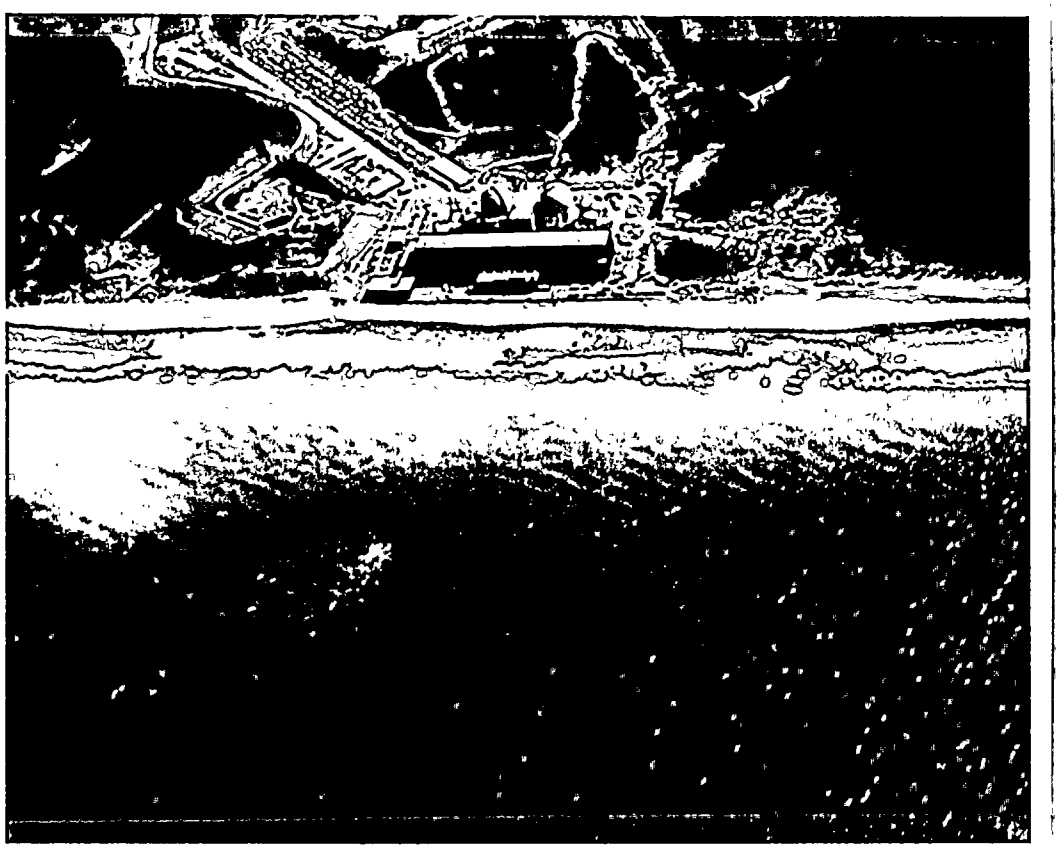

FIG. 2. Shore ice condition at Cook Plant on 16 March 1977. Outer ridge and lagoon ice deteriorating, inner (shoreward) ridges intact. The discharge plume shows as a whitish fan in the water lakeward of the left end of the plant buildings.

FIG. 3. View north to south along shore at Cook Plant on 16 March 1977 during spring melt-off. Deteriorating ice conditions at the plant, with similar ones in the distance far away from the plant. In the extreme distance all the ice has melted.

ICE CONDITIONS: CLIMATOLOGICAL DEPENDENCE 1976 (PRELIMINARY)

by

Erwin Seibel

May 1977

ICE CONDITIONS: CLIMATIOLOGICAL DEPENDENCE 1976 (PRELIMINARY)

The ice studies of the winter 1975-1976 at the Donald C. Cook Nuclear Plant were carried out in the same manner as those for the witners of 1973-74 and 1974-75 using a time lapse photographic system. The preliminary relationships between the ice conditions for the winter of 1975-76 and the climatological conditions are shown in the attached figures. An analysis of the information shows little if any variation in these relationships from those previously observed. It is noted that because of the relatively mild winter the period of ice cover and the extent of the ice cover during the winter of 1975-76 was significantly shorter and reduced.

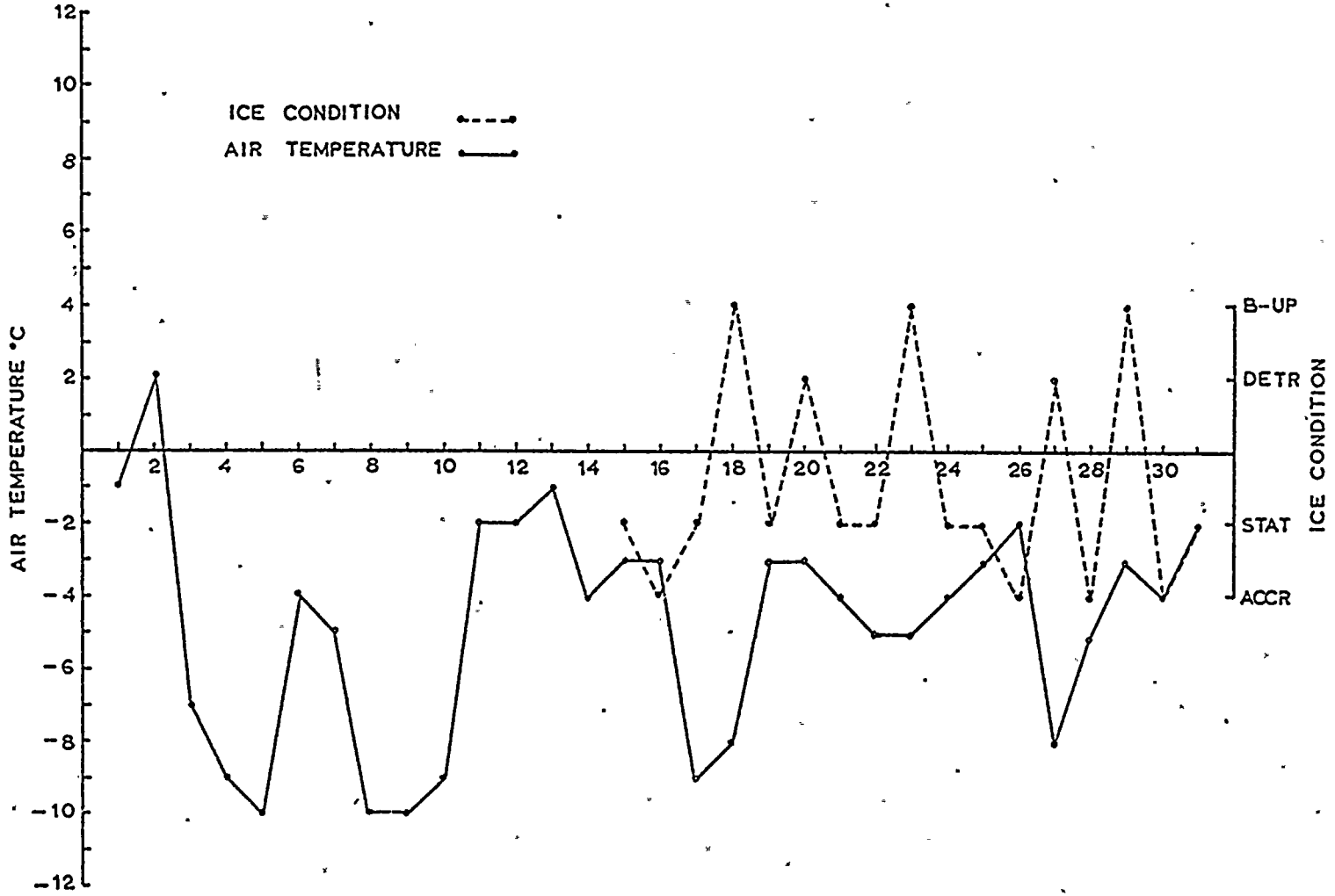

FIG. 1. Daily mean air temperature and ice conditions: January 1976

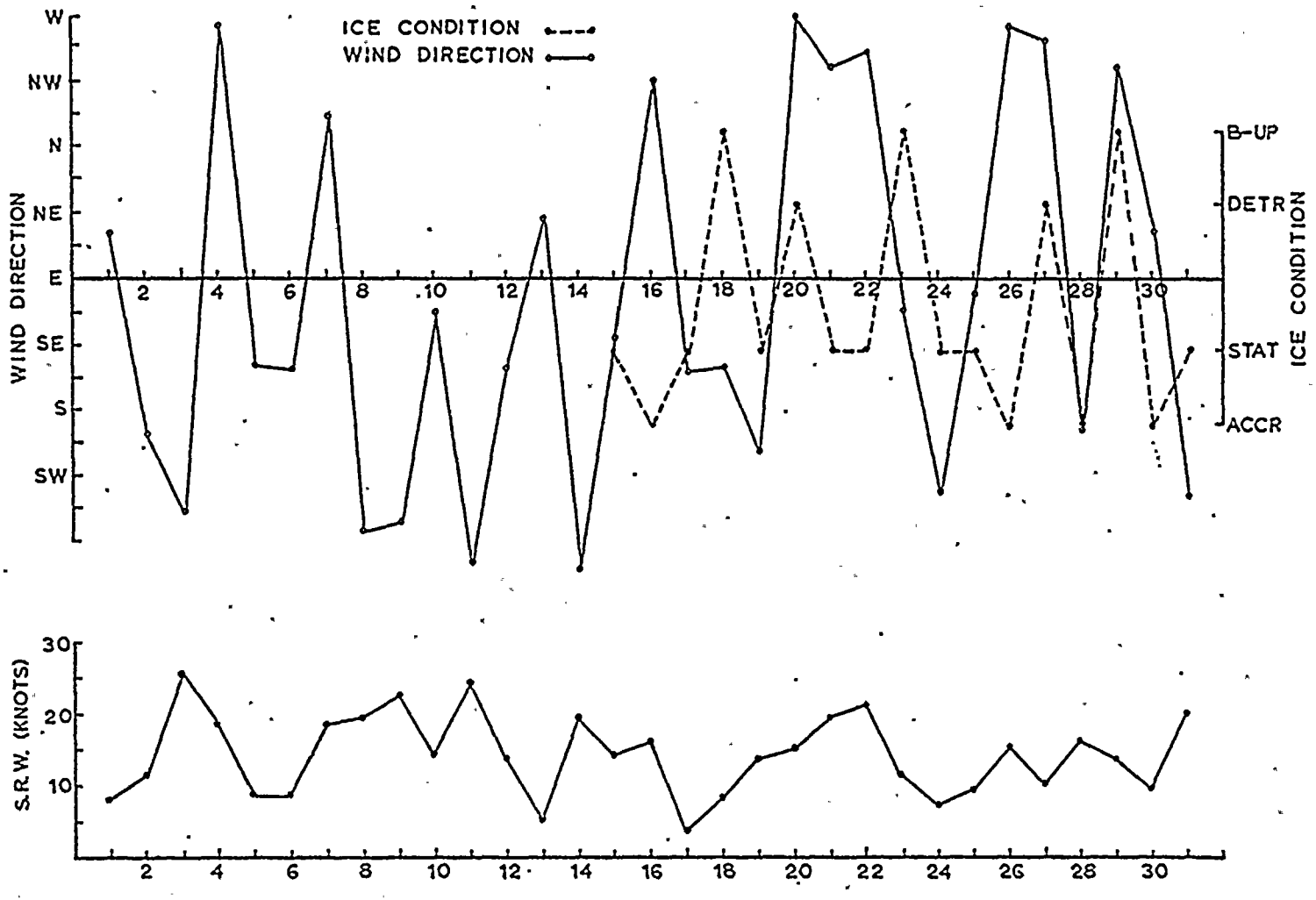

FIG. 2. Daily ice conditions vs. direction and speed of resultant wind: January 1976

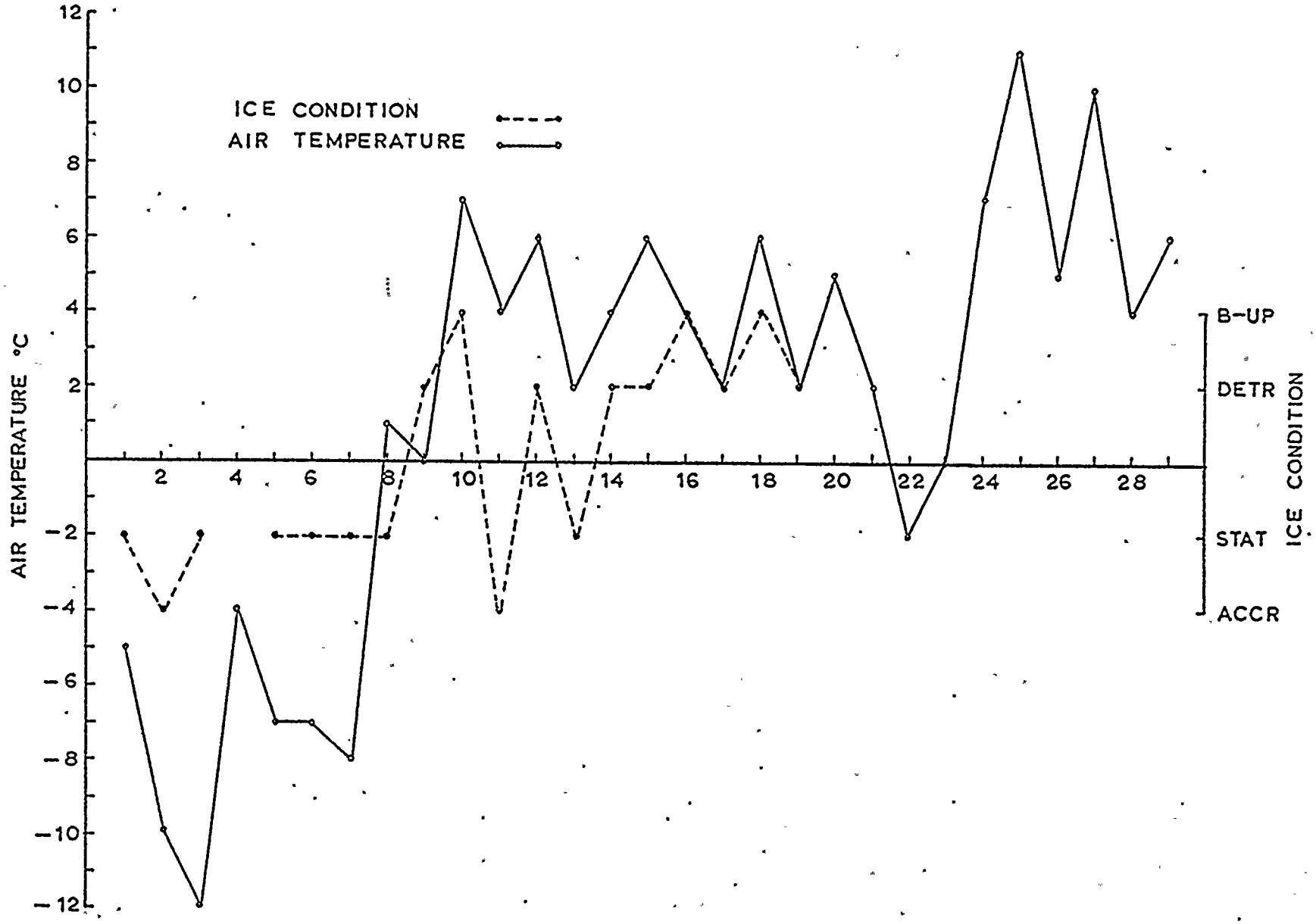

FIG. 3. Daily mean air temperature and ice conditions: February 1976

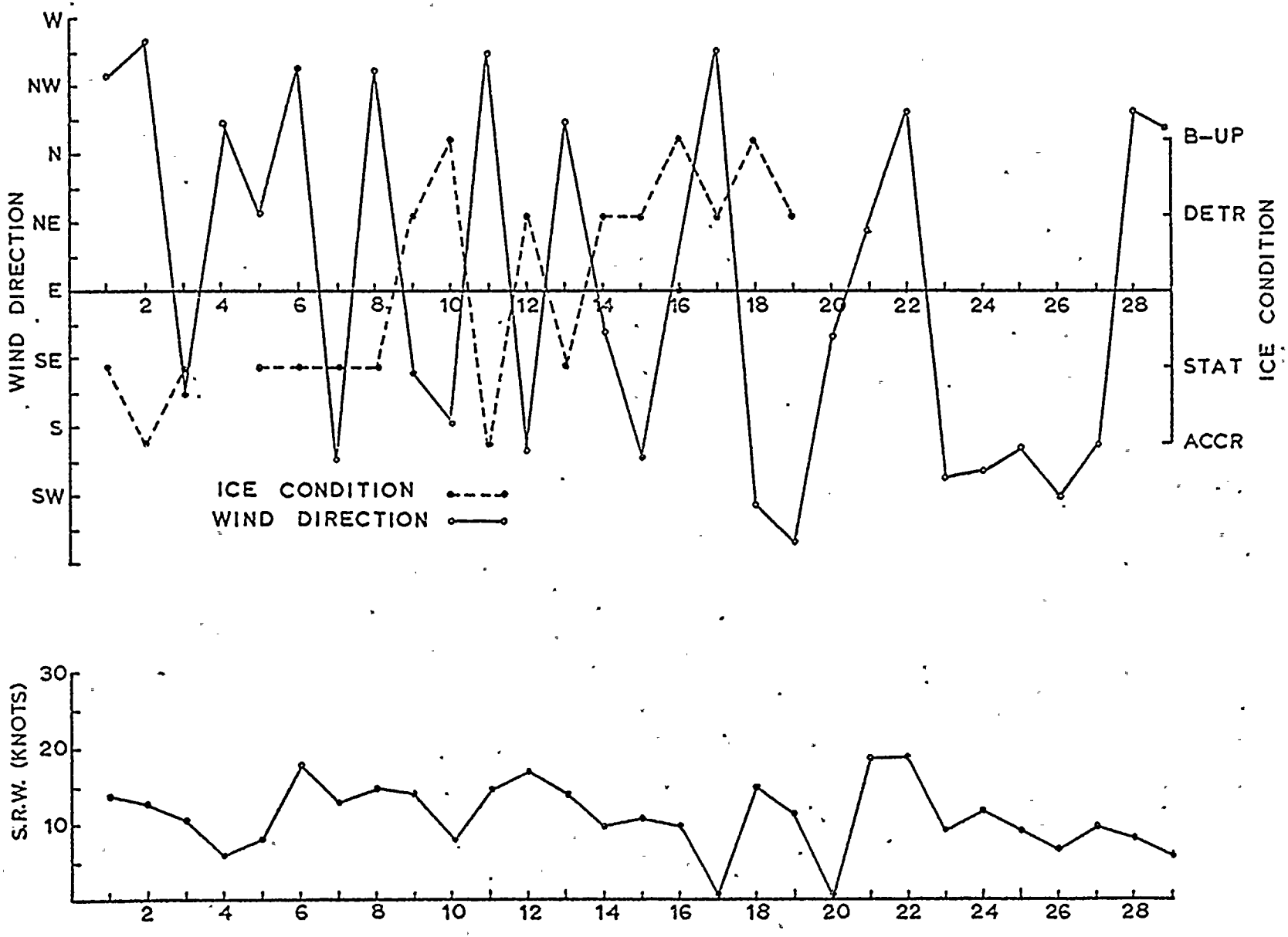

FIG. 4. Daily ice conditions vs. direction and speed of resultant wind: February 1976

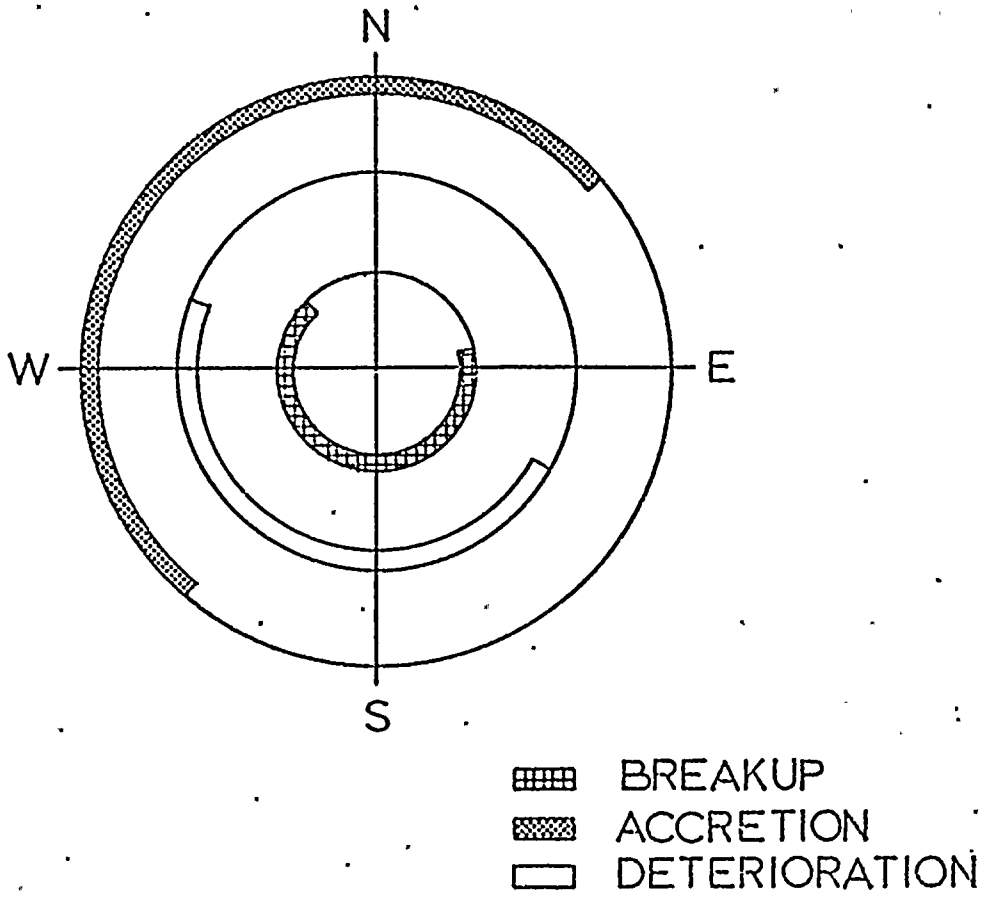

FIG. 5. Daily resultant wind direction vs. ice condition: January and February 1976 for winds with persistence of 75% or greater.